Sex-biased regulatory changes in the placenta of native highlanders contribute to adaptive fetal development

Tian Yue[1,4#], Yongbo Guo[1,4#], Xuebin Qi[1,2,3#], Wangshan Zheng[1#], Hui Zhang[1,3#], Bin Wang[2], Kai Liu[1], Bin Zhou[1,4], Xuerui Zeng[1,4], Ouzhuluobu[2], Yaoxi He[1]*, Bing Su[1,5]*

[1]State Key Laboratory of Genetic Resources and Evolution, Kunming Institute of Zoology, Chinese Academy of Sciences, Kunming 650223, China;

[2]Fukang Obstetrics, Gynecology and Children Branch Hospital, Tibetan Fukang Hospital, Lhasa 850000, China;

[3]State Key Laboratory of Primate Biomedical Research, Institute of Primate Translational Medicine, Kunming University of Science and Technology, Kunming, China.

[4]Kunming College of Life Science, University of Chinese Academy of Sciences, Beijing 100101, China;

[5]Center for Excellence in Animal Evolution and Genetics, Chinese Academy of Sciences, Kunming 650223, China;

[#]These authors contributed equally to this work.

***Corresponding authors**: Yaoxi He and Bing Su,

Email: heyaoxi@mail.kiz.ac.cn; sub@mail.kiz.ac.cn

Summary

Compared with lowlander migrants, native Tibetans have a higher reproductive success at high altitude though the underlying mechanism remains unclear. Here, we compared the transcriptome and histology of full-term placentas between native Tibetans and Han migrants. We found that the placental trophoblast shows the largest expression divergence between Tibetans and Han, and Tibetans show decreased immune response and endoplasmic reticulum stress. Remarkably, we detected a sex-biased expression divergence, where the male-infant placentas show a greater between-population difference than the female-infant placentas. The umbilical cord plays a key role in the sex-biased expression divergence, which is associated with the higher birth weight of the male newborns of Tibetans. We also identified adaptive histological changes in the male-infant placentas of Tibetans, including larger umbilical artery wall and umbilical artery intima and media, and fewer syncytial knots. These findings provide valuable insights into the sex-biased adaptation of human populations, with significant implications for medical and genetic studies of human reproduction.

Introduction

Hypobaric hypoxia at high altitude can restrict fetal growth, resulting in reduced neonatal birth weight (BW) and increased infant mortality (Moore et al., 2001b). Due to long-term natural selection at high altitude, native highlanders such as Tibetans have acquired a higher reproductive success than the lowlander migrants (e.g. Han Chinese moving to high altitude), reflected by the higher newborn BW and the lower prenatal and postnatal mortality (Beall et al., 2004; Moore et al., 2011). As expected, Tibetans performed better than Han migrants during fetal development (He et al., 2023; Julian et al., 2009; Moore et al., 2011; Moore et al., 2001a). Previous genomic studies have identified a group of genes potentially contributing to the genetic adaptation of Tibetans to high-altitude environments, and these studies were mostly focused on the blood and cardiopulmonary systems of adult Tibetans (Beall et al., 2010a; Bigham et al., 2010; Deng et al., 2019; Peng et al., 2017; Peng et al., 2011; Simonson et al., 2010; Song et al., 2020; Xiang et al., 2013; Xu et al., 2011; Yang et al., 2017; Yi et al., 2010). Although a recent study reported the association of more pregnancies and a higher survival birth rate based on GWAS analysis of 1,008 Nepali Tibetans, no adaptive genetic variant was identified (Jeong et al., 2018). Therefore, whether and how the Tibetan adaptive variants affect their fetal development and eventually improve the reproductive fitness are yet to be explored.

The placenta is a temporary organ that connects fetus to the mother's uterus during pregnancy, and it begins to develop around 6-7 days after gestation (Knofler et al., 2019). As an important organ of maternal-fetal exchange of nutrient, oxygen and waste, the placenta plays a critical role in fetal growth and development. Previous studies have reported that placental dysfunction can lead to premature birth, abnormal fetal growth and defects of neurological development (Guttmacher et al., 2014). At the same time, the genetic study reported that placental transcription in utero plays a key role in determining postnatal body size (Peng et al., 2018), and placenta weight is positively correlated with BW, an important trait related to the postnatal survival rate of newborns (Haeussner et al., 2013). Therefore, gene expression profiling of placenta

is essential to dissecting the molecular mechanism of the successful reproduction. Recently, a transcriptomic study comparing 91 placental samples (including 47 Tibetans giving birth at high altitudes) found that the genes related to autophagy and tricarboxylic acid cycle showed significant up-regulation in Tibetans. However, no lowlander migrants living at high altitude (>2500m) were included in this study (Wu et al., 2022).

In addition, it is known that the intrauterine growth rate of the male fetus is faster than that of the female fetus, and this growth rate difference leads to a higher proportion of preeclampsia, premature delivery and intrauterine growth restriction of the male fetus (Clifton, 2010). The between-sex difference of fetal development was explained by the higher transport efficiency, but weaker reserve capacity of the male fetal placenta (Eriksson et al., 2010). Consistently, we recently reported a male-biased pattern of BW seasonality in Tibetans and Han migrants living at high altitude. Compared to the female fetuses, the male fetuses are more sensitive to hypobaric hypoxia, reflected by their more serious BW reduction and relatively lower survival rates (He et al., 2022). However, whether the placenta plays a key role in the observed sex-biased sensitivity to hypoxia during fetal development at high altitude remains elusive.

In this study, we sampled 69 full-term placental tissues, including 35 native Tibetans and 34 Han migrants living at the same altitude (an elevation of 3,650m). Seven tissue layers of the placenta were dissected and analyzed in detail. With the use of RNA-seq, we generated a systematic map of placental transcriptomes of indigenous and migrant populations living at high altitude. Markedly, we found a male-biased transcriptomic divergence between Tibetans and Han migrants, and the gene expression pattern of the fetal umbilical cord may affect the BW of the male newborns. We also observed adaptive histological changes in the Tibetan male-infant placentas, providing further evidence on the sex-biased adaptation of fetal development.

Results

Gene expression profiles of placentas of native Tibetans and Han migrants

To understand the transcriptomic patterns of placentas of Tibetans and Han migrants at high altitude, we collected full-term (>37 weeks of gestation) placental samples from 35 Tibetans (16 male newborns and 19 female newborns) and 34 Han migrants (21 male newborns and 13 female newborns) with singleton birth. These Tibetan and Han migrant mothers live at the same high altitude (Lhasa, Tibet Autonomous Region, China; elevation = 3,650 m), and had experienced their entire pregnancy at this altitude. The population ancestry of the subjects was confirmed by self-claim, and further validated by the genome-sequencing data (**Methods, Figure S1**).

We first compared the newborn traits between the Tibetan group and the Han group. As expected, the average BW of the Tibetan newborns is significantly higher than that of the Han newborns (p=0.0121, unpaired Student's t-test), a clear indication of a better fetal development in Tibetans, while there are no significant differences in placental weight and placental volume (**Figure S2**). Given the placenta is a highly heterogeneous organs underlying functional and histological specializations in discrete anatomical parts (Sood et al., 2006), we dissected each placenta into seven tissue layers according to its anatomic structure (from fetal side to maternal side), including umbilical cord (UC), amnion (AN), chorion (CN), chorionic plate (CP), villus of fetal (VF), villus of intermediate (VI) and villus of maternal (VM), and we conducted RNA-seq of 483 placental samples (69 individuals × 7 layers) (**Figure 1A**), In total, ~12 billion short reads were generated. After applying a stringent quality control (**Methods**), we kept 448 placental transcriptome data, and each sample contains ~27 million reads on average (sample details in **Table S1**). In addition, we obtained the genome-wide variants of these mothers and their newborns from our previous studies (He et al., 2023; Zheng et al., 2023).

As the placenta is a maternal-fetal mosaic organ, we firstly determined the maternal-fetal compositions of each dissected layer using the genomic and

128 transcriptomic data (see **Methods** for details). The results show that UC and VF are
129 100% fetal origin, so are VM, VI, CP and AN (>95%) with tiny proportions of
130 maternal origin. By contrast, CN is mostly maternal origin (70%) (**Figure 1B**). This
131 pattern is consistent with the anatomic structure of the placenta (Sood et al., 2006).
132 Consequently, the RNA-seq data of placenta mostly represent the transcriptomes of
133 the newborns, except for the CN reflecting the mixed transcriptomes of mothers and
134 newborns.

135 The principal component analysis (PCA) indicates that the placental samples
136 cluster by layers instead of population groups, suggesting that the transcriptomic
137 difference between placental structures is greater than the between-population
138 divergence. This pattern is in line with previous transcriptome of three-layer placentas
139 (chorion, amnion and decidua) of Nepali Tibetans, in which the samples were grouped
140 by tissue type instead of ethnicity (Wu et al., 2022). Notably, the four trophoblast
141 layers (CP, VF, VI and VM) cannot be clearly separated in the PCA map and they
142 form a large cluster. These four layers belong to the chorionic villus, the essential
143 structure in placenta (Wapner and Jackson, 1988). The UC, AN and CN layers form
144 three separate clusters (**Figure 1C**). Accordingly, the gene expression heat-map
145 analysis generates the same clustering pattern (**Figure 1D**). These results suggest that
146 different layers of the placenta have distinct gene expression profiles, which can
147 provide detailed regulatory information in understanding the role of placenta in fetal
148 development.

149 **VF and VI show the largest expression divergence between Tibetans and Han**

150 To gain insights into the differences of gene expression in placenta between
151 Tibetans and Han, we performed differential gene expression analysis of the seven
152 placental layers (see **Methods** for technical details). In total, we identified 579
153 differentially expressed genes (DEGs) between Tibetans and Han, accounting for 3.4%
154 of the total number of expressed genes. Our results show that VF and VI have the
155 largest numbers of DEGs between Tibetans and Han (305 DEGs in VI and 173 DEGs
156 in VF), accounting for 82.56% (478/579) of the total DEGs in the placenta. By

contrast, the numbers of DEGs in the other five layers are much less (8-46 DEGs) (**Figure 2A, Table S2**). Notably, most of the DEGs (399/579, 68.91%) are detected in only one layer (**Figure 2A**), an indication of a layer-specific differential expression pattern. The results of GO enrichment analyses show that for VF and VI, and the top functional terms reflect an enhancement of mRNA regulation and a decrease of immune response (indicated by the terms of defense response to virus) in VF of Tibetans compared to Han (**Figure 2B, Table S3**). In VI, the significant functional terms (decreased expression in Tibetans) are mostly related to proteins targeting endoplasmic reticulum (ER) (**Figure 2B, Table S3**). Taken together, these results indicate that the differences between Tibetans and Han are mostly unfolded in the VF and VI layers, and Tibetans have less hypoxia-induced immune response and ER stress in the placenta (Elvekrog and Walter, 2015; Plumb et al., 2015; Tenzing et al., 2021). We did not see significant enrichment terms in the other layers due to the small numbers of DEGs.

There are 85 shared DEGs among the placental layers. As expected, most of them are two-layer shared DEGs between VF and VI (76/85, 89.41%), and the other 9 are multi-layer-shared DEGs (**Figure 2C**). In particular, there are two four-layer shared DEGs, and the two involved genes are *KCNE1* (potassium voltage-gated channel subfamily E regulatory subunit 1) and *AC004057.1*. *KCNE1* is significantly up-regulated in all four trophoblast layers (CP, VF, VI and VM) of Tibetans compared to Han (**Figure 2D**), and it is also the top up-regulated DEG in both VF and VI (**Figure 2E**). It encodes a potassium ion voltage-gated channel protein. The expression of *KCNE1* is reportedly down-regulated in preeclampsia placentas (Mistry et al., 2011), and the *in vitro* experiment also showed its down-regulation in the cultured cells under hypoxia (Luo et al., 2013). Therefore, the relative up-regulation of *KCNE1* in Tibetans is presumably beneficial to the reproductive outcomes at high altitude. The function of *AC004057.1* is currently unknown.

For the down-regulated genes in Tibetans, the top genes in VF and VI are *PADI1* (peptidyl arginine deiminase 1) and *TAC3* (tachykinin precursor 3), respectively

186 (**Figure 2E**). *PADI1* is a VF-specific DEG with 3.4-fold lower expression in Tibetans
187 compared to Han (p = 0.0001) (**Figure S3**). *PADI1* encodes a member of the peptidyl
188 arginine deiminase family enzymes. The expression of *PADI1* is triggered by hypoxia
189 and it stimulates *PKM2* activity and contributes to the increased glycolysis under
190 hypoxic condition (Coassolo et al., 2021). *TAC3* is a VI-VF-shared DEG with both >
191 3-fold changes in the two layers (Tibetans lower than Han, p = 0.04 for VI, and p =
192 0.04 for VF) (**Figure S3**). *TAC3* encodes a member of the tachykinin family of
193 secreted neuropeptides, and its high expression can lead to preeclampsia (Page et al.,
194 2006) and severe fetal growth restriction (Whitehead et al., 2013). Hence, the
195 observed down-regulation of these two genes suggests that compared to the Han
196 migrants, the placenta of Tibetans is more adapted to hypoxic environment,
197 presumably with a low level of hypoxia-induced glycolysis and a reduced risk of fetal
198 growth restriction.

199 **Sex-biased expression divergence in the placenta between Tibetans and Han**

200 Given the male fetuses are more sensitive to high-altitude hypoxia than the
201 female fetuses as described in our previous report (He et al., 2022), we next analyzed
202 the placental transcriptomes by taking into account of the infant gender (**Methods**).
203 When the gender identity is superimposed onto the PCA map in **Figure 1D**, we did
204 not see any clustering patterns by genders, implying that the gender-related expression
205 changes do not cause a dramatic profile shift (**Figure S4**). However, surprisingly, we
206 found a striking difference in view of the numbers of DEGs (Tibetans vs. Han), where
207 the male-fetus placentas have many more DEGs than the female-fetus placentas (759
208 genes vs. 31 genes), and there is no intersection between them (**Figure 3A**). This
209 between-sex difference is also reflected by the shared DEGs between the
210 gender-combined DEG set and the gender-separated DEG sets, where the male set has
211 128 shared DEGs, but only 5 shared DEGs in the female set (**Figure S4**), suggesting
212 that the male-fetus placentas contribute more to the detected between-population
213 expression divergence.

214 Of the 759 male-fetus DEGs, 728 DEGs are detected in one-layer. There are 25

215 two-layer-shared DEGs, 4 three-layer-shared DEGs and 2 four-layer-shared DEGs
216 (**Figure S5**). By contrast, there is no multi-layer shared DEGs in the female-fetus
217 placentas. Among the 31 layer-shared DEGs in the male-fetus placentas, 22 DEGs are
218 up-regulated and 9 DEGs are down-regulated in Tibetans. Similar to the above results,
219 there are a large portion of overlap between the layer-shared DGEs of the male-fetus
220 placentas and the gender-combined placentas (**Figure S5**).

221 Layer-wise, in the male-fetus placentas, UC, AN and VF have the largest numbers
222 of DEGs (396, 177 and 189, respectively, **Figure 3A, Table S4**), accounting for 95.49%
223 (762/798) of all DEGs, while the DEGs in the other layers are much less (< 15). By
224 contrast, the great majority of the DEGs in the female-fetus placentas is from UC (23
225 genes, **Table S5**), while the other layers only have a few DEGs (< 5). This DEG
226 pattern is highly different from that seen in the gender-combined result (**Figure 2A**),
227 again, an indication of a sex-biased expression divergence between Tibetans and Han
228 migrants at high altitude. Similar with the gender-combined result, the great majority
229 (>95% in both males and females) of the DEGs are one-layer DEGs. Given the
230 previous studies have been mostly focused on the functional role of the placental villi
231 (Lorca et al., 2021; Tana et al., 2021; Vaughan et al., 2020), our gender-separated
232 analyses illustrate the importance of UC and AN in fetal development, especially for
233 the male fetus.

234 Markedly, in the gender-combined result, we only detected 31 DEGs in the UC
235 layer, contrasting the large number of DEGs (396 genes) in the male-fetus placentas.
236 We found that this might be caused by the large portion of DEGs (248/396, 62.62%)
237 with an opposite direction of between-population expression divergence in the males
238 and females, respectively (**Figure S6**), which canceled out the differences in the
239 gender-combined analysis. Consistently, the between-sex expression comparison
240 (DEGs between genders in a population: Tibetan male vs. female; Han male vs.
241 female) indicates that the UC shows the largest DEG count difference between native
242 Tibetans and Han migrants (**Figure 3B** and **Figure S6**). Consequently, the UC layer
243 shows the most pronounced gender-dependent expression divergence.

The sex-biased expression divergence in placenta is likely caused by the differential responses of male and female fetuses to hypoxic stress at altitude, as proposed in our previous study (He et al., 2022). In UC, AN and VF, where the largest numbers of DEGs were detected in the male placentas, the top-5 DEGs are indicated in **Figure 3C**. These genes are primarily involved in immune responses, embryonic development, cell migration and cholesterol metabolism, all of which are closely related to fetal development (Barlan et al., 2017; Choi et al., 2019; Sifakis et al., 2018; Yang et al., 2021). In UC, the enriched GO terms include up-regulation of cytoplasmic translational initiation and DNA-binding transcription factor activity, and down-regulation of presynaptic endocytosis in Tibetans (**Figure 3D, Table S3**). In AN, Tibetans show a down-regulation in alcohol metabolic related process, phospholipid metabolic process and cholesterol biosynthetic process (**Figure 3D, Table S3**). These enriched functional categories reflect a more active protein synthesis and a reduced risk of hypoxia-induced metabolic disturbance, which are presumably beneficial to fetal development of the Tibetan male newborns (Guzel et al., 2017; Yung et al., 2008; Zhang et al., 2017). We did not see significant functional terms in VF (**Table S3**).

It is known that hypoxia can lead to inhibition of global protein synthesis and activation of ER stress (Koumenis, 2006). Our results suggest that compared to native Tibetans, the Han migrants are more responsive to hypoxic stress, reflected by their relative down-regulation of translational initiation and transcription factor activity, and this trend is mostly exemplified in the UC layer of the male placentas since UC is the key channel of maternal-fetal exchange of oxygen and nutrition. On the other hand, cholesterol plays an important role in embryonic development (Cortes et al., 2014). We detected the down-regulation of a cholesterol regulating gene (*DHCR7*) in Tibetans (**Figure 3C**). The *DHCR7*-encoded protein can covalently link to *Shh* (sonic hedgehog) to participate in brain, limb and genital development (Roux et al., 2000). Accumulation of *DHCR7* and deficiency in cholesterol production will cause a devastating developmental disorder (Prabhu et al., 2016).

Gene expression changes in the umbilical cord are associated with birth weight of the male newborns

As a critical organ for maternal-fetal nutrition and oxygen exchanges, the physiological status of the placenta is closely related to the neonatal status. We performed Weighted Gene Co-expression Network Analysis (WGCNA) to investigate the association between gene expression modules and the newborn-related traits. The investigated traits include birth weight (BW), biparietal diameter (BPD), femur length (FL), gestation time (GT), placental weight (PW), placental volume (PLV), abdominal girth (AG), amniotic fluid maximcon depth (AFMD), amniotic fluid (AFI), fetal heart rate (FH) and fundal height (FUH).

A total of 136 and 161 molecular modules were obtained from the placentas of the male infants and the female infants, respectively. We define a module as a significantly differential module (SDM) when the gene expression of a module is significantly correlated to population divergence (Tibetans vs. Han, $p < 0.05$) and the newborn-related traits ($p < 0.05$) (see **Methods** for details). Totally, there are 10 SDMs in males, but only 4 in females (**Figure 4A, Tables S6-9, Methods**). Markedly, the UC layer of the male infants has 3 SDMs, including Module 4 ($R = 0.39$, $p = 0.03$), Module 8 ($R = -0.45$, $p = 8.6\times10^{-3}$) and Module 9 ($R = -0.47$, $p = 6.4\times10^{-3}$) (**Figure 4A**), which are significantly associated with two newborn traits (BW and PLV), supporting a close involvement of UC in fetal development, especially for the male fetuses. There are four AN SDMs, two VF SDMs and one VI SDM that are associated with five newborn traits, including AFI (Module 16, Module 31 and Module 36), AFMI (Module 16 and Module 31), FUH (Module 18), AG (Module 95 and Module 96), and FH (Module 109), respectively (**Figure 4A**). For the female placentas, four SDMs are associated with AG (Module 107), AFMD (Module 45), FH (Module 45) and FUH (Module 34), respectively (**Figure 4A**). These identified SDMs suggest that the difference of transcriptional regulation of the placental layers between Tibetans and Han migrants do have impact on the newborn status, especially on the male infants.

302 We next looked at the DEGs in the SDMs. For the male placentas, there are a lot
303 of DEGs involved in the ten SDMs. By contrast, among the four SMDs in the female
304 placentas, there is only one DEG (**Figure 4B**). This pattern is consistent with the
305 male-biased gene expression divergence between Tibetans and Han. In particular, in
306 the UC layer of the male placentas, there are 196 DEGs in Module 8, and 104 DEGs
307 in Module 4. Most of the DEGs in Module 8 are down-regulated in the UC layer of
308 Tibetans (**Figure 4C**), and this module is negatively correlated with BW (**Figure 4B**
309 and **Figure S7**), indicating that the down-regulated gene expression module in the UC
310 layer of the Tibetan male placentas may contribute to the higher BW of the Tibetan
311 newborns compared to Han. There are 7 hub genes in Module 8, and all of them are
312 down-regulated in the Tibetan male placentas (**Figure 4C, 4D**). For example,
313 *SNRNP70* (small nuclear ribonucleoprotein U1 subunit 70) enables U1 snRNA
314 binding activity, and it is one of the known hypoxia-inducible target genes (Kurihara
315 et al., 2016). *TSC2* (TSC complex subunit 2) is a tumor suppressor gene that encodes
316 the growth inhibitory protein tuberin. Inhibition of the mTOR pathway by hypoxia
317 requires *TSC2*, leading to cell proliferation under hypoxia (Brugarolas et al., 2004).
318 Hence, the down-regulation of the great majority of DEGs in Module 8 suggests that
319 the male fetuses are likely more sensitive to hypoxic stress than the female fetuses,
320 and compared to native Tibetans, they are more responsive in the Han migrants,
321 which is associated with the higher BW in the adapted natives (Tibetans) compared to
322 the acclimatized migrants (Han). Taken together, the above results indicate that the
323 UC layer plays a key role in the development of the male fetus and ultimately affects
324 BW.

325 *GHR* (growth hormone receptor) is the only DEG in the SDMs of the female
326 newborns (**Figure 4B**). The gene expression level of *GHR* in the VF layer is
327 positively correlated with FUH (R = 0.44, p = 0.017) of the female newborns, an
328 indicator of fetal growth (Morse et al., 2009), but not the male newborns (**Figure S7**).
329 Consistently, it is up-regulated in Tibetans, corresponding to the higher FUH in
330 Tibetans (He et al., 2023). Interestingly, the expression pattern of *GHR* mirrors *GH*

331 (growth hormone) in placenta early development and embryonic growth (Harvey and
332 Baudet, 2014).

333 **Histological outcomes of the sex-biased expression divergence**

334 To further test the impact of the observed sex-biased expression divergence, we
335 performed histological examination of the UC, VF and VI where the most prominent
336 sex-biased expression and the largest numbers of DEGs were detected (**Figure 5A**).
337 We analyzed 20 individual placenta samples (male-infants: 5 Tibetans vs. 5 Han;
338 female-infants: 5 Tibetans vs. 5 Han). For the UC, five parameters of UC were
339 evaluated using cross-sections, including umbilical vein lumen (UVL), umbilical vein
340 wall (UVW), umbilical artery lumen (UAL), umbilical artery wall (UAW) and
341 umbilical artery intima and media (UAIM) (**Methods**).

342 In line with the expression data, we observed an obvious sex-biased histological
343 differences in UC, and the values of UVW and UAIM are significantly larger in
344 Tibetan male infants than Han ($p = 0.003$ and $p = 0.03$), but no differences seen in the
345 female infants ($p > 0.05$) (**Figure 5B, 5C**). The previous study reported a significant
346 association between preeclampsia and a smaller thickness and wall area of the
347 umbilical vein and artery, independent of gestation time and birth weight (Herzog et
348 al., 2017), which explains the presumably adaptive histological changes of UC
349 (increased UVM and UAIM) in Tibetans. No significant differences between Tibetans
350 and Han were observed in the other UC parameters (**Figure S8**).

351 For placental trophoblast (VF and VI), we counted the number of villi and
352 syncytial knots in the placenta (**Methods**). In the male placentas, Tibetans have more
353 villi in the VI layer than Han ($p < 0.0001$, **Figure 5D**), and the same trend was seen in
354 the VF layer though not significant ($p = 0.13$, **Figure S8**). Moreover, when we
355 counted the syncytial knots in the villi, we saw a significantly lower ratio of syncytial
356 knots/villi in male placenta of Tibetans ($p < 0.0001$, **Figure 5E**), an indication of
357 healthier villi because the appearance of syncytial knots are the degenerating feature
358 of placenta with remarkable accumulations of nuclei and degenerating organelles

359 (Heazell et al., 2007). By contrast, no difference was detected in the placentas of the
360 female newborns in view of the number of villi and the ratio of syncytial knots/villi in
361 either the VI layer or the VF layer (**Figure 5D, 5E** and **Figure S8**).

362 These sex-biased histological results are consistent with the patterns seen in gene
363 expression. The male infants show remarkably more DEGs between native Tibetans
364 and Han migrants than female infants, especially those genes involved in immune
365 responses. Also, our results prove that such male-biased expression divergence is
366 closely associated with birth weight. Therefore, as a distinctive remodeling of the UC
367 in male infants, the male-biased histological differences between Tibetans and Han
368 Chinese is most likely induced by the different inflammatory responses and
369 intrauterine hemodynamics. For placenta trophoblast, the difference of the syncytial
370 knots/villi ratios between VF and VI may be caused by their differences in the
371 distribution of placental villi. Branches of umbilical artery pass from the CP layer
372 before producing stem villi inferiorly (Castellucci et al., 1990). The VF layer is next
373 to the CP layer and the increased villus number in Tibetans suggests that the stem villi
374 extending out from umbilical artery produce more villous branches, which is
375 presumably beneficial to the maternal-fetal material exchange in Tibetans.
376 Consistently, the reduced number of syncytial knots in the VI layer of Tibetans might
377 be conducive to a better material exchange efficiency (Fogarty et al., 2013).

378 **Natural selection acts on the placental DEGs with expression divergence between**
379 **Tibetans and Han**

380 Given the overall gene expression divergence in the placenta between Tibetans
381 and Han migrants can explain the better newborn traits of Tibetans, the involved
382 genes could be the target of natural selection. At the same time, most of the adaptive
383 variants identified in Tibetan population are located in the noncoding regions of the
384 genome, suggesting the functional outcomes of these genetic variations are likely
385 achieved by gene expression regulation.

386 To see whether the detected DEGs of placenta tissues are subject to Darwinian
387 positive selection, therefore contributing to the genetic adaptation of reproductive

388 fitness in Tibetans, we checked all the identified DEGs and see whether they were
389 listed in the 192 reported Tibetan selection-nominated genes (TSNGs), i.e. the genes
390 showing signatures of Darwinian positive selection in Tibetans (Zheng et al., 2023).
391 In total, we found that 13 DEGs are TSNGs, including 4 DEGs from the
392 gender-combined gene list and 9 DEGs from the male-only gene list. No DEGs from
393 the female-only gene list is overlapped with the TSNGs (**Figure 6A**). Permutation test
394 shows that the overlapped DEGs with TSNGs are over-represented in the genome,
395 especially for the male-only DEGs (p = 9e-4) (**Figure S9**). Among the four DEGs
396 with selection signals in the gender-combined gene list, we saw *EPAS1*, the gene with
397 the strongest signal of selection in Tibetans, and it shows a significant
398 down-regulation in the UC layer of Tibetans compared to Han migrants (p = 0.04)
399 (**Figure 6B**). Previously, there were multiple SNPs of *EPAS1* with reported GWAS
400 signals for BW in lowland populations with a large sample size (N > 300,000)
401 (Warrington et al., 2019). Therefore, the down-regulation of *EPAS1* in the Tibetan
402 placentas likely reflects a blunted hypoxic response that may improve vasodilation of
403 UC for better blood flow, and eventually leading to the higher BW in Tibetans.

404 *FOXJ3* and *HSD11B1* are the other two genes overlapped between the placenta
405 DEGs and the TSNG set (**Figure 6B**). *FOXJ3* (Forkhead Box J3) is a transcriptional
406 activator, and reportedly plays an important role in spermatogenesis (Ni et al., 2016).
407 We observed a significant correlation of *FOXJ3* expression of the CN layer with
408 placenta weight and BW (p = 0.02 and p = 0.004, respectively) (**Figure S10**),
409 suggesting a potential role of *FOXJ3* in transcription regulation underlying early fetal
410 development. *HSD11B1* (Hydroxysteroid 11-Beta Dehydrogenase 1) is a microsomal
411 enzyme that catalyzes the conversion of the inactive hormone cortisol to the active
412 metabolite cortisone. The Tibetan placentas show a lower *HSD11B1* expression than
413 Han migrants (p = 0.01), which may bring a lower cortisol stress hormone level.
414 Given the hypoxia-induced glucocorticoid elevation can have impact on placental
415 vascular development and nutrient transport (Ozmen et al., 2017), the lower cortisol
416 stress hormone level in the Tibetan placentas might be advantageous under hypobaric

417 hypoxia at high altitude.

418 Among the nine DEGs with selection signals from the male-only gene list, four
419 are DEGs of the UC layer, including *EGLN1*, *L3MBTL2*, *MKL1* and *TRABD* (**Figures**
420 **6C and S11** and **Table S10**). *EGLN1* is one of the TSNGs with strong signals of
421 selection in Tibetans, and it is a member of the HIF (hypoxia induced factor) pathway
422 and works together with *EPAS1* (Peng et al. 2011). There are two Tibetan-enriched
423 missense mutations in the *EGLN1* gene, and the mutations are reportedly related to
424 the lower erythropoiesis and augmented hypoxic ventilatory response in Tibetans
425 (Lorenzo et al., 2014; Song et al., 2020). *EGLN1* is temporally expressed in an
426 oxygen-dependent fashion, with the greatest mRNA expression at 10-12 week of
427 gestation (Ietta et al., 2006). In the UC layer, we detected a significant
428 down-regulation of *EGLN1* in the Tibetan male placentas (p = 0.01), but not in the
429 Tibetan female placentas (p = 0.91) (**Figure 6C**). Among the other three genes, *MKL1*
430 (myocardin related transcription factor A, also named *MRTFA*) was reportedly
431 involved in vasoconstriction mediated by human vein endothelial cells under hypoxia
432 (Yang et al., 2013), and it possesses a series Tibetan-enriched SNPs and structural
433 variants (Ouzhuluobu et al., 2020; Zheng et al., 2023). The rat gene knockout model
434 indicated that a *MKL1* deletion could improve hypoxia induced pulmonary
435 hypertension (Yuan et al., 2014), and the Tibetan-enriched 163-bp deletion at *MKL1* is
436 associated with the lower pulmonary arterial pressure of Tibetans (Ouzhuluobu et al.,
437 2020). Therefore, the down-regulation of *MKL1* in the male placentas likely works in
438 the same way as *EGLN1* and *EPAS1* do, and may help reduce the risk of hypoxia
439 induced hypertension in Tibetans. In addition, *L3MBTL2* (L3MBTL histone
440 methyl-lysine binding protein 2) is involved in DNA damage response (Nowsheen et
441 al., 2018), and cell proliferation and differentiation (Markus et al., 2003). The
442 function of *TRABD* (TraB domain containing) is not known. More functional data are
443 needed to understand the adaptive roles of these genes in fetal development at high
444 altitude. Except for the DEGs of the UC layer, two DEGs of the AN layer (*ACSS2* and
445 *STXBP3*) and three DEGs of the VF layer (*ZNF160*, *FOXP1* and *ENDOU*) are also

446 overlapped with the TSNG set (**Figure S11**). These genes are mainly involved in the
447 functions about embryonic development, cardiac valve morphology and immune
448 response (Hu et al., 2006; Kanda et al., 2005).

449 Furthermore, we tested the speculated polygenic effect on the adaptation of gene
450 expression using eQTL (expression quantitative trait loci) in Tibetans (**Methods**). The
451 PolyGraph (Racimo et al., 2018) detected a significant signature of polygenic
452 selection on gene expression in Tibetans (adjusted $p = 0.003$) (**Figure S12**).
453

454 ## Discussion

455 The placenta is the key organ for fetal development, and the transcriptional
456 profiles of the placenta are highly informative in revealing the gene expression
457 patterns and the regulatory networks, which eventually contribute to the newborn
458 health. In this study, with a placental transcriptomic and histological profiling of
459 native Tibetans and Han migrants living at the same high altitude, we intend to dissect
460 the molecular mechanism of the observed higher reproductive fitness of Tibetans and
461 to understand how the gene expression regulation in the placenta explains the genetic
462 adaptation of Tibetans in view of fetal development, the determinant outcome of
463 natural selection.

464 We show that among the 7 anatomic layers of the placenta, VF and VI display
465 the largest expression divergence between Tibetans and Han migrants, which is
466 expected given the known crucial role of the placental trophoblast in fetal
467 development (Kingdom et al., 2000). The down-regulated DEGs in VF and VI of
468 Tibetans (compared to Han) are mainly involved in immune response and ER stress. It
469 is known that besides of the maternal-fetal exchanges of nutrient, oxygen and waste,
470 the placenta is also an important immune organ, and the immune response is one of
471 the physiological reactions under chronic hypoxia (Facco et al., 2005). Placental
472 hypoxia/ischemia can lead to the release of a variety of placental factors, the
473 activation of circulating immune cells and autoantibodies, and have a profound impact
474 on blood flow and arterial pressure regulation (Zarate et al., 2014). Hence, our results

475 suggest that Tibetans might acquire the ability of overcoming the hypoxia-induced
476 inflammation and ER stress protein translation inhibition at high altitude.

477 It is known that the sex of the fetus has a detectable impact on the developmental
478 status (Clifton, 2010), and maternal hypoxia could alter placental formation in a sex
479 specific manner in rodents (Cuffe et al., 2014). In addition, sex differences in
480 placental traits are reportedly associated with high elevation adaptation in Andeans
481 (Jackson et al., 1987). However, previous studies on human placenta did not take the
482 fetus's gender into account in gene expression analyses. In this study, by looking at
483 the transcriptomic profiles of the male and female placentas separately, we discovered
484 a striking pattern of a male-biased expression divergence between Tibetans and Han
485 migrants. By contrast, there is almost no difference in placental gene expression of the
486 female newborns between Tibetans and Han migrants. This result suggests that the
487 male placenta is more sensitive to environmental stresses such as hypobaric hypoxia
488 at altitude, and consequently, the expression divergence between Tibetans and Han
489 migrants is more pronounced in males.

490 In particular, the UC layer possesses the largest number of DEGs (396 genes) in
491 the male placentas, and the enriched functional categories of these DEGs imply a
492 more active protein synthesis and a reduced risk of hypoxia-induced metabolic
493 disorder in Tibetans. UC is the main channel of maternal-fetal exchange. Previous
494 studies have shown that UC is important for blood vitamin D (Alp et al., 2016) and
495 oxygen transportation (Postigo et al., 2009; Yancey et al., 1992). We speculate that
496 UC may play a key role in the differential development of the male fetus between
497 Tibetans and Han migrants, reflected by the three detected male-specific molecular
498 modules that ultimately affect BW. In addition, in the UC layer, the between-sex
499 expression comparison indicates that the expression differences between the male
500 placentas and the female placentas are more pronounced in Han migrants (117 DEGs)
501 compared to Tibetans (33 DEGs) (**Figure S6**). Hence, under hypoxic stress, besides of
502 the known important functions of the trophoblast layers of the placenta, UC and the
503 other non-trophoblast layers are also crucial, especially for the development of the

504 male fetus. This observation serves as an important guiding information for future
505 placental research.

506 Furthermore, at the histological level, we also see the male-biased differences
507 between Tibetans and Han migrants (**Figure 5**). The UC and VI/VF show distinctive
508 histological changes only in the male infants, the phenotypic outcome of the observed
509 sex-biased expression divergence between Tibetans and Han migrants. The UC and
510 fetal vasculature share the same embryonic origin, and vessels are often used as an
511 important index reflecting newborn vascular health (Jin and Patterson, 2009). We
512 observed that the umbilical artery wall and artery intima and media are significantly
513 larger in the Tibetan male infants than in Han, consistent with the previous report that
514 native Tibetans can prevent hypoxia-associated IUGR accompanied with the higher
515 uteroplacental blood flow in pregnancy (Moore et al., 2004). It is known that the UC
516 is highly influenced by systemic and local hemodynamic conditions of pregnancy,
517 such as blood flow, oxygen tension and oxidative stress (Blanco et al., 2011).
518 Preeclampsia is a complex disease characterized by an increased maternal blood
519 pressure during pregnancy and increased risks of fetal growth restriction and preterm
520 birth (Duley, 2009). It was reported that environmental hypoxia of high altitude
521 impairs fetal growth, increases the incidence of preeclampsia, and, as a result,
522 significantly increases the risk of perinatal and/or maternal morbidity and mortality
523 (Julian, 2011). Additionally, the histological and morphological studies reported that
524 the preeclampsia is associated with a smaller UC vein area and wall thickness
525 (Herzog et al., 2017; Inan et al., 2002). Therefore, our observation of the larger
526 umbilical artery wall and umbilical artery intima and media suggest that native
527 Tibetans might benefit from a remolding of the UC vessels, due to the decreased
528 expression of inflammation-related genes in the Tibetan placentas. Eventually,
529 Tibetans have achieved a higher uteroplacental blood flow, a lower prevalence of
530 preeclampsia, a higher newborn birth weight and a lower mortality at high altitude.
531 Notably, all these adjustments are more significant in the male infants than in the
532 female infants.

533 The adaptive changes are also reflected in the placental trophoblast. The VF and
534 VI layers are the substantial parts of placental villi, which are composed of
535 trophoblastic villi and are responsible for the exchange of nutrients and active
536 transportation. Syncytial knot is a specialized structure of trophoblastic villi, which
537 increases with fetal age and is a feature of placenta maturity (Loukeris et al., 2010). It
538 is reportedly increased in the placenta of eclampsia and fetal growth restriction. In
539 vitro experiments have proved that syncytial knots can be induced by hypoxia and
540 other stressful conditions (Heazell et al., 2007). In the Tibetan male placentas, there
541 are fewer syncytial knots compared to Han migrants, likely resulting from the
542 observed male-biased expression changes. More functional data is needed to establish
543 the mechanistic connection between the expression profiles and the histological
544 outcomes.

545 As the gene with the strongest signal of natural selection in Tibetans, *EPAS1* has
546 been reported in numerus studies on its contribution to high altitude adaptation. In this
547 study, we detected a significant expression reduction of *EPAS1* in the Tibetan UC
548 compared to the high-altitude Han. It was reported that the selected-for *EPAS1*
549 variants/haplotype were associated with lower hemoglobin levels in the Tibetan
550 highlanders with a major effect (Beall et al., 2010; Peng et al., 2017), and the low
551 hemoglobin concentration of Tibetans is causally associated with a better reproductive
552 success (Cho et al., 2017). Therefore, we speculate that the selective pressure on
553 *EPAS1* is likely through its effect on hemoglobin, rather than directly on the
554 reproductive traits. The down-regulation of *EPAS1* in placenta likely reflects a blunted
555 hypoxic response that may improve vasodilation of UC for better blood flow, and
556 eventually leading to the higher BW in Tibetans (He et al., 2023). For *EGLN1*,
557 another well-known gene in Tibetans, we detected between-population expression
558 difference in the male UC layer, but not in other placental layers. Considering the
559 known adaptation mechanism of *EGLN1* is attributed to the two Tibetan-enriched
560 missense mutations, the contribution of *EGLN1* to the gene expression change in the
561 Tibetan UC was unexpected and worth to be explored in the future.

562 It should be noted that there are limitations in our study. We only analyzed the
563 full-term placentas. At this stage, the placenta has fully matured and we may not be
564 able to capture the dynamic changes during earlier placental and fetal development.
565 Also, we did include placenta data of a low-elevation reference, and we could not
566 completely rule out the possible effect of random genetic drift on gene expression
567 divergence between populations, which is not due to adaptation in Tibetans.
568 Additionally, although we have identified four DEGs (Tibetans vs. Han migrants)
569 with reported signals of Darwinian positive selection (Zheng et al., 2023), the
570 transcriptome data is insufficient to explain the underlying molecular mechanisms of
571 genetic adaptation in Tibetans. Future single-cell transcriptome analysis and
572 functional validations of the candidate genes are warranted to reveal the responsible
573 cell types and the molecular pathways.

574 In summary, we present a comprehensive analysis of transcriptional profiles and
575 histological differences of placentas of Tibetans and Han migrants. Our data suggest
576 that the male fetuses are more sensitive to high-altitude hypoxia, and the UC layer
577 plays a key role in the male-biased transcriptional divergence of the placenta between
578 Tibetans and Han migrants, suggesting its important role in the higher reproductive
579 fitness of Tibetans as the outcome of intense natural selection at high altitude.

580 Materials and methods

581 Ethical Approval

582 All participants signed the written informed consent. To make sure the local
583 native Tibetans can fully understand the content of the consent, the informed consent
584 was prepared in two language versions (Chinese and Tibetan), and we provided oral
585 interpretation for those who were not able to read. The protocol of this study was
586 reviewed and approved by the Internal Review Board of Kunming Institute of
587 Zoology, Chinese Academy of Sciences (Approval ID: SMKX-20160311–45) and the
588 research scheme is in accordance with the Regulations of the People's Republic of
589 China on the Administration of Human Genetic Resources.

590 **Sample collection and processing**

591 We collected 69 healthy full-term placental samples at a hospital in Lhasa
592 (elevation = 3,650 m), the capital of Tibet Autonomous Region, China. The detailed
593 information of the investigated samples and statistic results were provided in Tables
594 S11 and S12. Based on the anatomic structure and the published protocol (Sood et al.,
595 2006), each placenta was divided into seven tissue layers, from fetal side to maternal
596 side, including umbilical cord (UC), amnion (AN), chorion (CN), chorionic plate (CP),
597 villus of fetal (VF), villus of intermediate (VI) and villus of maternal (VM). The UC
598 layer was dissected by cutting approximately 4 cm from the placental insertion point.
599 The AN and CN layers were obtained by stripping. We sampled AN from the area
600 approximately 5 cm from the placental insertion point and CN from the area 3 cm
601 from the placental junction. We obtained the placental parenchyma ~2.5 cm thick at ~
602 3 cm from the placental insertion point. After separation of CP, the remaining part was
603 dissected into triplicates of equal thickness: the maternal layer (including the thin
604 basal plate), the intermediate layer, and the fetal layer. Tissues were snap frozen in
605 liquid nitrogen and stored at -80℃. Part of the placenta tissue samples were also
606 subject to OCT (optimal cutting temperature compound) embedding for tissue section
607 analysis. All placental samples were obtained and stored within two hours of delivery.
608 The information of population ancestry of the sampled subjects was collected by
609 self-claim with no recorded admixture in the past three generations, which was further
610 validated by the genome-sequencing data (Zheng et al. 2023).

611 **RNA extraction and sequencing**

612 Total RNA of the placental samples was extracted using TRIzol reagent, and
613 RNA purity was determined using agarose gel electrophoresis and NanoDrop 2000
614 (Thermo Scientific). After RNA extraction, we assessed the RNA integrity and purity
615 using agarose gel electrophoresis. The RIN value of the extracted RNA was 7.56 ±
616 0.71. The extracted RNA was stored at -80℃. RNA library construction and
617 sequencing were conducted through commercial service (Novogene). The Illumina
618 HiSeq 2500 platform was utilized to sequencing with paired-end 150 bp reads. We

obtained >6G raw sequencing data for each sample.

Read alignment and quality control

In total, we generated 483 placental RNA-seq data from 69 full-term deliveries of Tibetans (35 placentas) and Han migrants (34 placentas). The quality controls (QCs) including following criteria: 1) filter out low-quality reads; 2) remove the sequence with low quality ends (the applied threshold was 30); 3). Trim reads embracing the joint sequences and the sequences containing the ambiguous base N; 4) remove the transcripts of each sample with reads length < 60. After QCs, we obtained a high-quality clean data for subsequent analyses.

The reference human genome (GRCh38 version) and annotation file were downloaded from the *ensemble* database (http://www.ensembl.org/index.html), and the clean reads were then mapped to the reference genome using STAR release 2.6.1a (Dobin et al., 2013) with the following default parameters "*--runThreadN 8 --readFilesCommand gunzip –c –outSAMtype BAM SortedByCoordinate –outSAMmapqUnique 60 --outSAMattrRGline ID:sample SM:sample PL:ILLUMINA --outSAMmultNmax 1 --outSJfilterReads Unique --outFilterMismatchNmax 2 --alignIntronMin 20 --alignIntronMax 50000 --sjdbOverhang 149 --quantMode TranscriptomeSAM GeneCounts --twopassMode Basic*". The position information of the sequencing reads on the reference genome and the feature information of each sample were obtained to create bam files. Subsequently, the bam files were fed to the *resm* software (https://github.com/deweylab/RSEM) (Li and Dewey, 2011) to generate read counts and TPM (transcripts per million reads). In total, 10.6 billion reads were mapped to the annotated regions, and 17,283 genes express in all the investigated placenta.

Determination of fetal and maternal origin of placenta

To trace the maternal-fetal origin of the placenta, we calculated the maternal and fetal ratio by using the maternal genomic data and the fetal genome-array data. An informative SNP is defined as fetal-specific when it is heterozygous in fetus (A/B)

647 and meanwhile is homozygous in mother (A/A) (Tsang et al., 2017).
648 Maternal-specific informative SNP definition is opposite. We randomly selected fetal
649 specific and mother specific tag SNP (at least 5 informative SNPs for each sample),
650 respectively. B is the specific allele and A is defined as common allele. For the
651 RNA-seq data of each layer of placental tissue, we calculate allelic ratio (R) according
652 to the following formula:

$$R = \frac{\mathrm{B}}{\mathrm{B} + \mathrm{A}}$$

653 We calculated five times and got five R values each sample, and calculated the
654 average value as maternal-specific allelic ratio (R_m) and fetal-specific allelic ratio (R_f)
655 of the sample.

656 **Differential expression analysis**

657 Differential expression analysis was performed by R package DESeq2 (Love et
658 al., 2014) on the seven layers of placenta. We added two covariates (fetal sex and
659 maternal age) to correct for gene expression: design = ~ fetal sex + maternal age. A
660 nominal significance threshold of the adjusted $p < 0.05$ was used to identify
661 differentially expressed genes (DEGs). The Benjamini-Hochberg FDR (false
662 discovery rate) procedure was used in multiple testing correction of p-values.
663 Functional enrichment analysis of DEGs was evaluated using the clusterProfiler (Yu
664 et al., 2012), we calculated the FDR-adjusted q-values from the overall p-values to
665 correct for multiple testing. For the gender-separated analysis of differential
666 expression, only maternal age was included in covariates.

667 **Construction of gene co-expression module**

668 We used R package WGCNA (Langfelder and Horvath, 2008) to construct gene
669 expression module for the male-infant placentas and the female-infant placentas
670 separately. The purpose of this analysis is to capture the interactions between gene
671 co-expression modules and reproductive phenotypes. The 11 reproductive phenotypes
672 were included: birth weight (BW), biparietal diameter (BPD), femur length (FL),
673 gestation (GT), placental weight (PW), placental volume (PLV), abdominal girth

(AG), amniotic fluid maximcon depth (AFMD), amniotic fluid (AFI), fetal heart (FH) and fundal height (FUH).

We used *varianceStabilizingTransformation* data from DESeq2 as input expression data. Use the *pickSoftThreshold* function to perform the analysis of network topology and choose a proper soft-thresholding power. Call *blockwiseModules* function to build gene network and identify modules. Then we correlated phenotypic characteristics with summary profile and look for the most significant associations. Considering there are 12 traits, we calculated a Bonferroni threshold (p-value = 0.05/number of independent traits) using the correlation matrix of the traits to evaluate the significant modules. The estimated the number of independent traits among the 12 investigated traits was 4. Therefore, we used a more stringent significant threshold of p-value = 0.0125 (0.05/4) as the final threshold to correct multiple testing brought by multiple traits in the WGCNA analysis.

Identification of key differential modules and hub genes

The module is defined differential when the p-value < 0.05 in population-based WGCNA analysis and p-value < 0.05 for phenotype-based WGCNA analysis. We defined a module as key differential modules when a differential module with the most significant p value, at the same time, with the most significant overlaps with DEGs. Co-expression gene networks were visualized using Cytoscape (v3.7.0) (Shannon et al., 2003). Functional enrichment analysis of genes in the modules of interest was performed using clusterProfiler.

We defined hub genes with three criteria: 1) gene module correlation > 0.2; 2) gene phenotype correlation > 0.8; 3) interaction degree ranked in the top 3.

Simulation analysis

We adopted the permutation approach to evaluate the enrichment of genes overlapped between DEGs and TSNGs. For each permutation, we randomly extracted 192 genes from the human genome, then overlapped them with the three DEG sets (female and male; female only; male only) and counted the gene number. After 10,000

702 permutations, we constructed a null distribution for each set, and found that the
703 overlapped genes between DEGs and TSNGs were significantly enriched in the
704 "female and male" set (p = 0.048) and the "male" set (p = 9e-4), but not in the
705 "female" set (p = 0.1158) (**Figure S9**). This result suggests that the observed DEGs
706 were significantly enriched in TSNGs when compared to random sampling, especially
707 for the male DEGs.

708 **Analysis of polygenic adaptation**

709 We employed the PolyGraph (Racimo et al., 2018) tool to identify the signatures
710 of polygenic selection in Tibetans using eQTL information. We conducted eQTL
711 analysis for seven layers, and collected a set of 5,251 eQTLs, conversing the SNPs
712 associated with gene expression with a significant p-value < 5e-8. To obtain a list of
713 independent eQTLs, we removed those SNPs in linkage disequilibrium (r2 > 0.2 in
714 1000 Genome Project). Finally, we obtained 176 independent eQTLs. At the same
715 time, we generated a set of 1,308,436 independent SNPs of Tibetans as the control
716 panel.

717 **Histological analysis**

718 We performed histological analysis for three parts of placenta: UC, VF and VI,
719 and compared the differences between native Tibetans and Han migrants. In total, 20
720 individual placenta samples from random selection were analyzed, including 10 from
721 male infants (5 Tibetans vs. 5 Han) and 10 from female infants (5 Tibetans vs. 5 Han).
722 For the UC, we firstly fixed the UC tissue in 4% paraformaldehyde 48h after picked
723 out from -80°C freezer, then cut the middle part of the UC (~0.5cm long) and fixed
724 overnight. Next, the OCT embedding was performed after sucrose gradient
725 dehydration (15% sucrose dewatering bottling, 30% sucrose dewatering bottling, 4°C),
726 with the umbilical cord facing upward. Finally, we performed frozen section (10 μm
727 thickness) and H&E staining. Five parameters of UC were evaluated based on
728 published methods (Lan et al., 2018), including area size of umbilical vein lumen
729 (UVL), umbilical vein wall (UVW), umbilical artery lumen (UAL), umbilical artery

730 wall (UAW) and umbilical artery intima and media (UAIM). All these parameters
731 were analyzed by ImageJ (Collins, 2007). Considering lack of paraffin embedded
732 material, we placed OCT embedded tissue in 4% paraformaldehyde for fixation and
733 paraffin embedding. Then, the samples were cut into 0.3 μm thick sections and
734 counterstain to H&E staining. Five fields with equal area per section were randomly
735 selected for counting the numbers of villi and the numbers of syncytial knots, and the
736 average numbers was taken in the Tibetan-Han comparison.
737
738

Acknowledgements

We are grateful to all participants in this study. We would like to acknowledge Chunxia Li, Rongrong Bai and all other Doctors and Nurses from Obstetrical Department and Delivery Room of Fukang Obstetrics and Gynecology Children's Branch Hospital for their assistance in data collection of the pregnant cohorts.

Funding

This study was funded by grants from the National Natural Science Foundation of China (NSFC) (32288101 and 91631306 to B.S; 3217040584 and 32000390 to Y.H.; 32070578 and U22A20340 to X.Q and 32170629 to H.Z.), the Youth Innovation Promotion Association of CAS (to Y.H.), the Science and Technology General Program of Yunnan Province (202301AW070010 and 202001AT070110 to Y.H.), the Provincial Key Research, Development and Translational Program of Tibetan Autonomous Region of China (XZ202201ZY0035G to X.Q.), and the State Key Laboratory of Genetic Resources and Evolution (GREKF22-15 to H.Z.).

Author contribution

B.S., Y.H. designed the study. T.Y., Y.G., X.Q., W.Z., H.Z., Ouzhuluobu, B. W. collected the placenta samples and phenotypic data. T.Y., Y.G. performed the experiments. T.Y., Y.G., W.Z., Y.H., K.L., B.Z., X.Z. analyzed the data. B.S. supervised the project; T.Y., Y.H., B.S. wrote the manuscript with input from all authors.

Competing interests

Authors declare that they have no competing interests.

Data and materials availability

Transcriptome data and phenotypic data generated by this study are stored on GSA under the project ID of PRJCA014064. Additional material supporting this study is available from the corresponding authors upon request.

References

Alp, H., Tekgunduz, K.S., and Akkar, M.K. (2016). Maternal and cord blood vitamin D status in high-altitude pregnancy. J Matern Fetal Neonatal Med *29*, 571-575.

Barlan, K., Cetera, M., and Horne-Badovinac, S. (2017). Fat2 and Lar Define a Basally Localized Planar Signaling System Controlling Collective Cell Migration. Dev Cell *40*, 467-477 e465.

Beall, C.M., Cavalleri, G.L., Deng, L., Elston, R.C., Gao, Y., Knight, J., Li, C., Li, J.C., Liang, Y., McCormack, M.*, et al.* (2010a). Natural selection on EPAS1 (HIF2alpha) associated with low hemoglobin concentration in Tibetan highlanders. Proc Natl Acad Sci U S A *107*, 11459-11464.

Beall, C.M., Cavalleri, G.L., Deng, L.B., Elston, R.C., Gao, Y., Knight, J., Li, C.H., Li, J.C., Liang, Y., McCormack, M.*, et al.* (2010b). Natural selection on EPAS1 (HIF2 alpha) associated with low hemoglobin concentration in Tibetan highlanders. P Natl Acad Sci USA *107*, 11459-11464.

Beall, C.M., Song, K.J., Elston, R.C., and Goldstein, M.C. (2004). Higher offspring survival among Tibetan women with high oxygen saturation genotypes residing at 4,000 m. P Natl Acad Sci USA *101*, 14300-14304.

Bigham, A., Bauchet, M., Pinto, D., Mao, X., Akey, J.M., Mei, R., Scherer, S.W., Julian, C.G., Wilson, M.J., Lopez Herraez, D.*, et al.* (2010). Identifying signatures of natural selection in Tibetan and Andean populations using dense genome scan data. PLoS Genet *6*, e1001116.

Blanco, M.V., Vega, H.R., Giuliano, R., Grana, D.R., Azzato, F., Lerman, J., and Milei, J. (2011). Histomorphometry of umbilical cord blood vessels in preeclampsia. J Clin Hypertens (Greenwich) *13*, 30-34.

Brugarolas, J., Lei, K., Hurley, R.L., Manning, B.D., Reiling, J.H., Hafen, E., Witters, L.A., Ellisen, L.W., and Kaelin, W.G., Jr. (2004). Regulation of mTOR function in response to hypoxia by REDD1 and the TSC1/TSC2 tumor suppressor complex. Genes Dev *18*, 2893-2904.

Castellucci, M., Scheper, M., Scheffen, I., Celona, A., and Kaufmann, P. (1990). The development of the human placental villous tree. Anat Embryol (Berl) *181*, 117-128.

Cho, J.I., Basnyat, B., Jeong, C., Di Rienzo, A., Childs, G., Craig, S.R., Sun, J., and Beall, C.M. (2017). Ethnically Tibetan women in Nepal with low hemoglobin concentration have better reproductive outcomes. Evol Med Public Health *2017*, 82-96.

Choi, W.S., Lee, G., Song, W.H., Koh, J.T., Yang, J., Kwak, J.S., Kim, H.E., Kim, S.K., Son, Y.O., Nam, H.*, et al.* (2019). The CH25H-CYP7B1-RORalpha axis of cholesterol metabolism regulates osteoarthritis. Nature *566*, 254-258.

Clifton, V.L. (2010). Review: Sex and the human placenta: mediating differential strategies of fetal growth and survival. Placenta *31 Suppl*, S33-39.

Coassolo, S., Davidson, G., Negroni, L., Gambi, G., Daujat, S., Romier, C., and Davidson, I. (2021). Citrullination of pyruvate kinase M2 by PADI1 and PADI3 regulates glycolysis and cancer cell proliferation. Nat Commun *12*, 1718.

Collins, T.J. (2007). ImageJ for microscopy. Biotechniques *43*, 25-30.

Cortes, V.A., Busso, D., Maiz, A., Arteaga, A., Nervi, F., and Rigotti, A. (2014). Physiological and pathological implications of cholesterol. Front Biosci (Landmark Ed) *19*, 416-428.

Cuffe, J.S., Walton, S.L., Singh, R.R., Spiers, J.G., Bielefeldt-Ohmann, H., Wilkinson, L., Little, M.H., and Moritz, K.M. (2014). Mid- to late term hypoxia in the mouse alters placental morphology, glucocorticoid regulatory pathways and nutrient transporters in a sex-specific manner. J Physiol *592*, 3127-3141.

Deng, L., Zhang, C., Yuan, K., Gao, Y., Pan, Y., Ge, X., He, Y., Yuan, Y., Lu, Y., Zhang, X., *et al.* (2019). Prioritizing natural-selection signals from the deep-sequencing genomic data suggests multi-variant adaptation in Tibetan highlanders. Natl Sci Rev *6*, 1201-1222.

Dobin, A., Davis, C.A., Schlesinger, F., Drenkow, J., Zaleski, C., Jha, S., Batut, P., Chaisson, M., and Gingeras, T.R. (2013). STAR: ultrafast universal RNA-seq aligner. Bioinformatics *29*, 15-21.

Duley, L. (2009). The global impact of pre-eclampsia and eclampsia. Semin Perinatol *33*, 130-137.

Elvekrog, M.M., and Walter, P. (2015). Dynamics of co-translational protein targeting. Curr Opin Chem Biol *29*, 79-86.

Eriksson, J.G., Kajantie, E., Osmond, C., Thornburg, K., and Barker, D.J. (2010). Boys live dangerously in the womb. Am J Hum Biol *22*, 330-335.

Facco, M., Zilli, C., Siviero, M., Ermolao, A., Travain, G., Baesso, I., Bonamico, S., Cabrelle, A., Zaccaria, M., and Agostini, C. (2005). Modulation of immune response by the acute and chronic exposure to high altitude. Med Sci Sports Exerc *37*, 768-774.

Fogarty, N.M., Ferguson-Smith, A.C., and Burton, G.J. (2013). Syncytial knots (Tenney-Parker changes) in the human placenta: evidence of loss of transcriptional activity and oxidative damage. Am J Pathol *183*, 144-152.

Guttmacher, A.E., Maddox, Y.T., and Spong, C.Y. (2014). The Human Placenta Project: placental structure, development, and function in real time. Placenta *35*, 303-304.

Guzel, E., Arlier, S., Guzeloglu-Kayisli, O., Tabak, M.S., Ekiz, T., Semerci, N., Larsen, K., Schatz, F., Lockwood, C.J., and Kayisli, U.A. (2017). Endoplasmic Reticulum Stress and Homeostasis in Reproductive Physiology and Pathology. Int J Mol Sci *18*.

Haeussner, E., Schmitz, C., von Koch, F., and Frank, H.G. (2013). Birth weight correlates with size but not shape of the normal human placenta. Placenta *34*, 574-582.

Harvey, S., and Baudet, M.L. (2014). Extrapituitary growth hormone and growth? Gen Comp Endocrinol *205*, 55-61.

He, Y., Guo, Y., Zheng, W., Yue, T., Zhang, H., Wang, B., Feng, Z., Ouzhuluobu, Cui, C., Liu, K., *et al.* (2023). Polygenic adaptation leads to a higher reproductive fitness of native Tibetans at high altitude. Curr Biol.

He, Y., Li, J., Yue, T., Zheng, W., Guo, Y., Zhang, H., Chen, L., Li, C., Li, H., Cui, C., *et al.* (2022). Seasonality and Sex-Biased Fluctuation of Birth Weight in Tibetan Populations. Phenomics *2*, 64-71.

Heazell, A.E., Moll, S.J., Jones, C.J., Baker, P.N., and Crocker, I.P. (2007). Formation of syncytial knots is increased by hyperoxia, hypoxia and reactive oxygen species. Placenta *28 Suppl A*, S33-40.

Herzog, E.M., Eggink, A.J., Reijnierse, A., Kerkhof, M.A., de Krijger, R.R., Roks, A.J., Reiss, I.K., Nigg, A.L., Eilers, P.H., Steegers, E.A., *et al.* (2017). Impact of early- and late-onset preeclampsia on features of placental and newborn vascular health. Placenta *49*, 72-79.

Hu, H., Wang, B., Borde, M., Nardone, J., Maika, S., Allred, L., Tucker, P.W., and Rao, A. (2006). Foxp1 is an essential transcriptional regulator of B cell development. Nat Immunol *7*, 819-826.

Ietta, F., Wu, Y., Winter, J., Xu, J., Wang, J., Post, M., and Caniggia, I. (2006). Dynamic HIF1A regulation during human placental development. Biol Reprod *75*, 112-121.

Inan, S., Sanci, M., Can, D., Vatansever, S., Oztekin, O., and Tinar, S. (2002). Comparative morphological differences between umbilical cords from chronic hypertensive and preeclamptic pregnancies. Acta Med Okayama *56*, 177-186.

Jackson, M.R., Mayhew, T.M., and Haas, J.D. (1987). Morphometric studies on villi in human term placentae and the effects of altitude, ethnic grouping and sex of newborn. Placenta *8*, 487-495.

Jeong, C., Witonsky, D.B., Basnyat, B., Neupane, M., Beall, C.M., Childs, G., Craig, S.R., Novembre, J., and Di Rienzo, A. (2018). Detecting past and ongoing natural selection among ethnically Tibetan women at high altitude in Nepal. PLoS genetics *14*, e1007650.

Jin, S.W., and Patterson, C. (2009). The opening act: vasculogenesis and the origins of circulation. Arterioscler Thromb Vasc Biol *29*, 623-629.

Julian, C.G. (2011). High altitude during pregnancy. Clin Chest Med *32*, 21-31.

Julian, C.G., Wilson, M.J., and Moore, L.G. (2009). Evolutionary Adaptation to High Altitude: A View From In Utero. Am J Hum Biol *21*, 614-622.

Kanda, H., Tamori, Y., Shinoda, H., Yoshikawa, M., Sakaue, M., Udagawa, J., Otani, H., Tashiro, F., Miyazaki, J., and Kasuga, M. (2005). Adipocytes from Munc18c-null mice show increased sensitivity to insulin-stimulated GLUT4 externalization. J Clin Invest *115*, 291-301.

Kingdom, J., Huppertz, B., Seaward, G., and Kaufmann, P. (2000). Development of the placental villous tree and its consequences for fetal growth. Eur J Obstet Gynecol Reprod Biol *92*, 35-43.

Knofler, M., Haider, S., Saleh, L., Pollheimer, J., Gamage, T., and James, J. (2019). Human placenta and trophoblast development: key molecular mechanisms and model systems. Cell Mol Life Sci *76*, 3479-3496.

Koumenis, C. (2006). ER stress, hypoxia tolerance and tumor progression. Curr Mol Med *6*, 55-69.

Kurihara, T., Westenskow, P.D., Gantner, M.L., Usui, Y., Schultz, A., Bravo, S., Aguilar, E., Wittgrove, C., Friedlander, M., Paris, L.P.*, et al.* (2016). Hypoxia-induced metabolic stress in retinal pigment epithelial cells is sufficient to induce photoreceptor degeneration. Elife *5*.

Langfelder, P., and Horvath, S. (2008). WGCNA: an R package for weighted correlation network analysis. BMC Bioinformatics *9*, 559.

Li, B., and Dewey, C.N. (2011). RSEM: accurate transcript quantification from RNA-Seq data with or without a reference genome. BMC Bioinformatics *12*, 323.

Lorca, R.A., Houck, J.A., Laurent, L.C., Matarazzo, C.J., Baker, K., Horii, M., Nelson, K.K., Bales, E.S., Euser, A.G., Parast, M.M.*, et al.* (2021). High altitude regulates the expression of AMPK pathways in human placenta. Placenta *104*, 267-276.

Lorenzo, F.R., Huff, C., Myllymaki, M., Olenchock, B., Swierczek, S., Tashi, T., Gordeuk, V., Wuren, T., Ri-Li, G., McClain, D.A.*, et al.* (2014). A genetic mechanism for Tibetan high-altitude adaptation. Nat Genet *46*, 951-956.

Loukeris, K., Sela, R., and Baergen, R.N. (2010). Syncytial knots as a reflection of placental maturity: reference values for 20 to 40 weeks' gestational age. Pediatr Dev Pathol *13*, 305-309.

Love, M.I., Huber, W., and Anders, S. (2014). Moderated estimation of fold change and dispersion for RNA-seq data with DESeq2. Genome Biol *15*, 550.

Luo, Y., Kumar, P., and Mendelson, C.R. (2013). Estrogen-related receptor gamma (ERRgamma) regulates oxygen-dependent expression of voltage-gated potassium (K+) channels and tissue kallikrein during human trophoblast differentiation. Mol Endocrinol *27*, 940-952.

Markus, J., Feikova, S., Sramko, M., Wolff, L., and Bies, J. (2003). Proliferation-linked expression of the novel murine gene m4mbt encoding a nuclear zinc finger protein with four mbt domains. Gene *319*, 117-126.

Mistry, H.D., McCallum, L.A., Kurlak, L.O., Greenwood, I.A., Broughton Pipkin, F., and Tribe, R.M. (2011). Novel expression and regulation of voltage-dependent potassium channels in placentas from women with preeclampsia. Hypertension *58*, 497-504.

Moore, L.G., Charles, S.M., and Julian, C.G. (2011). Humans at high altitude: hypoxia and fetal growth.

Respir Physiol Neurobiol *178*, 181-190.
Moore, L.G., Shriver, M., Bemis, L., Hickler, B., Wilson, M., Brutsaert, T., Parra, E., and Vargas, E. (2004). Maternal adaptation to high-altitude pregnancy: an experiment of nature--a review. Placenta *25 Suppl A*, S60-71.
Moore, L.G., Young, D., McCullough, R.E., Droma, T., and Zamudio, S. (2001a). Tibetan protection from intrauterine growth restriction (IUGR) and reproductive loss at high altitude. Am J Hum Biol *13*, 635-644.
Moore, L.G., Young, D., McCullough, R.E., Droma, T., and Zamudio, S. (2001b). Tibetan protection from intrauterine growth restriction (IUGR) and reproductive loss at high altitude. Am J Hum Biol *13*, 635-644.
Morse, K., Williams, A., and Gardosi, J. (2009). Fetal growth screening by fundal height measurement. Best Pract Res Clin Obstet Gynaecol *23*, 809-818.
Ni, L., Xie, H., and Tan, L. (2016). Multiple roles of FOXJ3 in spermatogenesis: A lesson from Foxj3 conditional knockout mouse models. Mol Reprod Dev *83*, 1060-1069.
Nowsheen, S., Aziz, K., Aziz, A., Deng, M., Qin, B., Luo, K., Jeganathan, K.B., Zhang, H., Liu, T., Yu, J.*, et al.* (2018). L3MBTL2 orchestrates ubiquitin signalling by dictating the sequential recruitment of RNF8 and RNF168 after DNA damage. Nat Cell Biol *20*, 455-464.
Ouzhuluobu, He, Y., Lou, H., Cui, C., Deng, L., Gao, Y., Zheng, W., Guo, Y., Wang, X., Ning, Z.*, et al.* (2020). De novo assembly of a Tibetan genome and identification of novel structural variants associated with high-altitude adaptation. Natl Sci Rev *7*, 391-402.
Ozmen, A., Unek, G., and Korgun, E.T. (2017). Effect of glucocorticoids on mechanisms of placental angiogenesis. Placenta *52*, 41-48.
Page, N.M., Dakour, J., and Morrish, D.W. (2006). Gene regulation of neurokinin B and its receptor NK3 in late pregnancy and pre-eclampsia. Mol Hum Reprod *12*, 427-433.
Peng, S., Deyssenroth, M.A., Di Narzo, A.F., Cheng, H., Zhang, Z., Lambertini, L., Ruusalepp, A., Kovacic, J.C., Bjorkegren, J.L.M., Marsit, C.J.*, et al.* (2018). Genetic regulation of the placental transcriptome underlies birth weight and risk of childhood obesity. PLoS genetics *14*, e1007799.
Peng, Y., Cui, C., He, Y., Ouzhuluobu, Zhang, H., Yang, D., Zhang, Q., Bianbazhuoma, Yang, L., He, Y.*, et al.* (2017). Down-Regulation of EPAS1 Transcription and Genetic Adaptation of Tibetans to High-Altitude Hypoxia. Mol Biol Evol *34*, 818-830.
Peng, Y., Yang, Z., Zhang, H., Cui, C., Qi, X., Luo, X., Tao, X., Wu, T., Ouzhuluobu, Basang*, et al.* (2011). Genetic variations in Tibetan populations and high-altitude adaptation at the Himalayas. Mol Biol Evol *28*, 1075-1081.
Plumb, R., Zhang, Z.R., Appathurai, S., and Mariappan, M. (2015). A functional link between the co-translational protein translocation pathway and the UPR. Elife *4*.
Postigo, L., Heredia, G., Illsley, N.P., Torricos, T., Dolan, C., Echalar, L., Tellez, W., Maldonado, I., Brimacombe, M., Balanza, E.*, et al.* (2009). Where the O2 goes to: preservation of human fetal oxygen delivery and consumption at high altitude. J Physiol *587*, 693-708.
Prabhu, A.V., Luu, W., Sharpe, L.J., and Brown, A.J. (2016). Cholesterol-mediated Degradation of 7-Dehydrocholesterol Reductase Switches the Balance from Cholesterol to Vitamin D Synthesis. J Biol Chem *291*, 8363-8373.
Racimo, F., Berg, J.J., and Pickrell, J.K. (2018). Detecting Polygenic Adaptation in Admixture Graphs. Genetics *208*, 1565-1584.
Roux, C., Wolf, C., Mulliez, N., Gaoua, W., Cormier, V., Chevy, F., and Citadelle, D. (2000). Role of

cholesterol in embryonic development. Am J Clin Nutr *71*, 1270S-1279S.

Shannon, P., Markiel, A., Ozier, O., Baliga, N.S., Wang, J.T., Ramage, D., Amin, N., Schwikowski, B., and Ideker, T. (2003). Cytoscape: a software environment for integrated models of biomolecular interaction networks. Genome Res *13*, 2498-2504.

Sifakis, S., Androutsopoulos, V.P., Pontikaki, A., Velegrakis, A., Papaioannou, G.I., Koukoura, O., Spandidos, D.A., and Papantoniou, N. (2018). Placental expression of PAPPA, PAPPA-2 and PLAC-1 in pregnacies is associated with FGR. Mol Med Rep *17*, 6435-6440.

Simonson, T.S., Yang, Y., Huff, C.D., Yun, H., Qin, G., Witherspoon, D.J., Bai, Z., Lorenzo, F.R., Xing, J., Jorde, L.B.*, et al.* (2010). Genetic evidence for high-altitude adaptation in Tibet. Science *329*, 72-75.

Song, D., Navalsky, B.E., Guan, W., Ingersoll, C., Wang, T., Loro, E., Eeles, L., Matchett, K.B., Percy, M.J., Walsby-Tickle, J.*, et al.* (2020). Tibetan PHD2, an allele with loss-of-function properties. Proceedings of the National Academy of Sciences of the United States of America *117*, 12230-12238.

Sood, R., Zehnder, J.L., Druzin, M.L., and Brown, P.O. (2006). Gene expression patterns in human placenta. Proc Natl Acad Sci U S A *103*, 5478-5483.

Tana, W., Noryung, T., Burton, G.J., van Patot, M.T., and Ri-Li, G. (2021). Protective Effects from the Ischemic/Hypoxic Stress Induced by Labor in the High-Altitude Tibetan Placenta. Reprod Sci *28*, 659-664.

Tenzing, N., van Patot, M.T., Liu, H., Xu, Q., Liu, J., Wang, Z., Wang, Y., Wuren, T., and Ge, R.L. (2021). Identification of a miRNA-mRNA Regulatory Networks in Placental Tissue Associated With Tibetan High Altitude Adaptation. Front Genet *12*, 671119.

Tsang, J.C.H., Vong, J.S.L., Ji, L., Poon, L.C.Y., Jiang, P., Lui, K.O., Ni, Y.B., To, K.F., Cheng, Y.K.Y., Chiu, R.W.K.*, et al.* (2017). Integrative single-cell and cell-free plasma RNA transcriptomics elucidates placental cellular dynamics. Proc Natl Acad Sci U S A *114*, E7786-E7795.

Vaughan, O.R., Thompson, F., Lorca, R.A., Julian, C.G., Powell, T.L., Moore, L.G., and Jansson, T. (2020). Effect of high altitude on human placental amino acid transport. J Appl Physiol (1985) *128*, 127-133.

Wapner, R.J., and Jackson, L. (1988). Chorionic villus sampling. Clinical obstetrics and gynecology *31*, 328-344.

Warrington, N.M., Beaumont, R.N., Horikoshi, M., Day, F.R., Helgeland, O., Laurin, C., Bacelis, J., Peng, S., Hao, K., Feenstra, B.*, et al.* (2019). Maternal and fetal genetic effects on birth weight and their relevance to cardio-metabolic risk factors. Nat Genet *51*, 804-814.

Whitehead, C.L., Walker, S.P., Ye, L., Mendis, S., Kaitu'u-Lino, T.J., Lappas, M., and Tong, S. (2013). Placental specific mRNA in the maternal circulation are globally dysregulated in pregnancies complicated by fetal growth restriction. J Clin Endocrinol Metab *98*, E429-436.

Wu, D., Liu, Y., Chen, W., Shao, J., Zhuoma, P., Zhao, D., Yu, Y., Liu, T., Yu, R., Gan, Y.*, et al.* (2022). How Placenta Promotes the Successful Reproduction in High-Altitude Populations: A Transcriptome Comparison between Adaptation and Acclimatization. Molecular biology and evolution *39*.

Xiang, K., Ouzhuluobu, Peng, Y., Yang, Z., Zhang, X., Cui, C., Zhang, H., Li, M., Zhang, Y., Bianba*, et al.* (2013). Identification of a Tibetan-specific mutation in the hypoxic gene EGLN1 and its contribution to high-altitude adaptation. Molecular biology and evolution *30*, 1889-1898.

Xu, S., Li, S., Yang, Y., Tan, J., Lou, H., Jin, W., Yang, L., Pan, X., Wang, J., Shen, Y.*, et al.* (2011). A genome-wide search for signals of high-altitude adaptation in Tibetans. Mol Biol Evol *28*, 1003-1011.

Yancey, M.K., Moore, J., Brady, K., Milligan, D., and Strampel, W. (1992). The effect of altitude on umbilical cord blood gases. Obstet Gynecol *79*, 571-574.

Yang, F., Whelan, E.C., Guan, X., Deng, B., Wang, S., Sun, J., Avarbock, M.R., Wu, X., and Brinster, R.L. (2021). FGF9 promotes mouse spermatogonial stem cell proliferation mediated by p38 MAPK signalling. Cell Prolif *54*, e12933.

Yang, J., Jin, Z.B., Chen, J., Huang, X.F., Li, X.M., Liang, Y.B., Mao, J.Y., Chen, X., Zheng, Z., Bakshi, A.*, et al.* (2017). Genetic signatures of high-altitude adaptation in Tibetans. Proc Natl Acad Sci U S A *114*, 4189-4194.

Yang, Y., Chen, D., Yuan, Z., Fang, F., Cheng, X., Xia, J., Fang, M., Xu, Y., and Gao, Y. (2013). Megakaryocytic leukemia 1 (MKL1) ties the epigenetic machinery to hypoxia-induced transactivation of endothelin-1. Nucleic Acids Res *41*, 6005-6017.

Yi, X., Liang, Y., Huerta-Sanchez, E., Jin, X., Cuo, Z.X.P., Pool, J.E., Xu, X., Jiang, H., Vinckenbosch, N., Korneliussen, T.S.*, et al.* (2010). Sequencing of 50 Human Exomes Reveals Adaptation to High Altitude. Science *329*, 75-78.

Yu, G.C., Wang, L.G., Han, Y.Y., and He, Q.Y. (2012). clusterProfiler: an R Package for Comparing Biological Themes Among Gene Clusters. Omics *16*, 284-287.

Yuan, Z., Chen, J., Chen, D., Xu, G., Xia, M., Xu, Y., and Gao, Y. (2014). Megakaryocytic leukemia 1 (MKL1) regulates hypoxia induced pulmonary hypertension in rats. Plos One *9*, e83895.

Yung, H.W., Calabrese, S., Hynx, D., Hemmings, B.A., Cetin, I., Charnock-Jones, D.S., and Burton, G.J. (2008). Evidence of placental translation inhibition and endoplasmic reticulum stress in the etiology of human intrauterine growth restriction. Am J Pathol *173*, 451-462.

Zarate, A., Saucedo, R., Valencia, J., Manuel, L., and Hernandez, M. (2014). Early disturbed placental ischemia and hypoxia creates immune alteration and vascular disorder causing preeclampsia. Arch Med Res *45*, 519-524.

Zhang, R., Dong, S., Ma, W.W., Cai, X.P., Le, Z.Y., Xiao, R., Zhou, Q., and Yu, H.L. (2017). Modulation of cholesterol transport by maternal hypercholesterolemia in human full-term placenta. Plos One *12*, e0171934.

Zheng, W., He, Y., Guo, Y., Yue, T., Zhang, H., Li, J., Zhou, B., Zeng, X., Li, L., Wang, B.*, et al.* (2023). Large-scale genome sequencing redefines the genetic footprints of high-altitude adaptation in Tibetans. Genome Biol *24*, 73.

1019 **Figure legends**

1020

1021 **Figure 1. Sampling strategy and gene expression patterns of the placental layers**
1022 **of Tibetans and Han migrants at high altitude. (A)** The strategy of sampling the
1023 full-term placentas. The placenta was dissected into seven layers, as shown from the
1024 fetal side to the maternal side, are umbilical cord (UC), amnion (AN), chorion (CN),
1025 chorionic plate (CP), villus of fetal (VF), villus of intermediate (VI) and villus of
1026 maternal (VM). The seven layers are labeled with seven different colors. **(B)** Analysis
1027 of the maternal-fetal origins of the placental layers. **(C)** The map of principal
1028 component analysis (PCA) showing the clustering pattern of placental tissue layers.
1029 **(D)** The heat map of gene expression in the seven placental layers of Tibetans and
1030 Han migrants reveals the same clustering pattern seen in the PCA map. The layers are
1031 color-coded (see panel-A).

1032

1033 **Figure 2. The gene expression differences of the placental layers between**
1034 **Tibetans and Han migrants**. **(A)** The numbers of differentially expressed genes
1035 (DEGs) between Tibetans and Han in each placenta layer; Purple: the number of
1036 up-regulated DEGs in Tibetans; Green: the number of down-regulated DEGs in
1037 Tibetans; The pie chart indicates the shared DEGs among two and more placental
1038 layers. **(B)** The enriched functional categories (GO terms) of the up-regulated (top)
1039 and the down-regulated (bottom) DEGs in VF and VI, respectively. The dashed line
1040 denotes the threshold of significant test (adjusted p-value < 0.05). **(C)** The heat map
1041 of the 85 shared DEGs among two and more placental layers. **(D)** Comparison of the
1042 expression levels of *KCNE1* between Tibetans and Han in the seven layers of placenta.
1043 The significant between-population differences are indicated. adjusted p-value (p):
1044 *-$p < 0.05$; **-$p < 0.01$; ***-$p < 0.001$. **(E)** The volcano plots of the DEGs in VF and
1045 VI, respectively. The top genes are indicated.

1046

1047 **Figure 3. Sex-biased placental expression divergence between Tibetans and Han**
1048 **migrants**. **(A)** The DEG numbers of the seven placental layers in the male infants and
1049 the female infants, respectively. Left: female (pink); Right: male (blue); Venn chart:
1050 the overlapped DEGs between male-infant placentas and female-infant placentas. **(B)**
1051 Bar plot show the difference of gene counts between cross-sex DEGs in native
1052 Tibetans and Han migrants. **(C)** The up- and down-regulated genes in the male infants
1053 of Tibetans compared to Han, shown in the volcano plots of UC, AN and VF; The
1054 top-5 DEGs are indicated. The example gene *DHCR7* is highlighted in red. **(D)** The

1055 enriched functional categories (GO terms) of the up-regulated (purple) and the
1056 down-regulated (green) DEGs in UC and AN, respectively. The dashed line denotes
1057 the threshold of significant test (adjusted *p*-value < 0.05).

1058

1059 **Figure 4. Gene expression modules in UC of the male infants correlate with**
1060 **neonatal phenotypes. (A)** The heat maps of *p*-values showing the correlations
1061 between gene expression and the newborn traits of the male-infant placentas (left) and
1062 the female-infant placentas (right). Inner ring: module name; Outer ring: layers; Red:
1063 significantly differential modules (SDMs). **(B)** The counts of the module-associated
1064 DEGs in the seven placental layers of the male infants and the female infants (the
1065 upper panels), and their correlations with the newborn traits (the lower panels). **(C)**
1066 The gene co-expression network of Module 8 of the male infants. **(D)** Gene
1067 expression comparisons of two hub genes in UC of the male infants between Tibetans
1068 and Han.

1069

1070 **Figure 5. Sex-biased histological changes in the male-infant placentas of Tibetans.**
1071 **(A)** Schematic diagram of the sampling strategy in histological analysis. **(B)(C)** The
1072 H&E stained cross-sections of the UC vessels (umbilical vein (UV); panel B; and
1073 umbilical artery (UA); panel C). The umbilical vein wall (UVW) and umbilical artery
1074 intima and media (UAIM) are highlighted in red. The boxplots show the comparisons
1075 of area size of UVW and UAIM between Tibetan and Han male infants (left) or
1076 female infants (right). The two umbilical arteries of each umbilical cord were subject
1077 to analysis in Panel-C. **(D)(E)** The H&E stained sections of the placental VI and VF.
1078 The arrows denote the syncytial knots. The boxplots show the comparison of the villi
1079 numbers or the syncytial knot/villi ratios between Tibetan and Han male infants (left)
1080 or female infants (right). Unpaired Student's t-tests are used to evaluate the
1081 significance of difference. *, *p*-value < 0.05; **, *p*-value < 0.01; ns, not significant.

1082

1083 **Figure 6. The differentially expressed genes in the placenta that underwent**
1084 **positive selection in Tibetans. (A)** The Venn plots show the intersections between the
1085 placental DEGs and the 192 Tibetan selection-nominated genes (TSNGs), covering
1086 the gender-combined and the gender-separated DEGs. **(B)** The three DEGs
1087 (gender-combined) under positive selection in Tibetans. The upper panels show the
1088 allele frequencies of variants with the strongest signals of selection within the gene.
1089 Besides of Tibetans and Han Chinese, the data from three other reference populations
1090 are also presented, including Japanese (JPT), Europeans (CEU) and Africans (YRI)

from the 1000 Genome Project. The solid and hollow bars in red denote the allele frequencies in the published 1001 Tibetan individuals and 35 Tibetan individuals, respectively, and the solid and hollow bars in blue denote the allele frequencies in the published 103 Han individuals and 34 Han individuals, respectively. The bottom panels show the comparison of the expression levels between Tibetans and Han in the seven layers of placenta. Only the significant between-population differences are indicated. adjusted *p*-value: *, *p*-value < 0.05; **, *p*-value < 0.01; ***, *p*-value < 0.001. **(C)** The three DEGs (gender-separated analysis) with signals of positive selection in Tibetans.

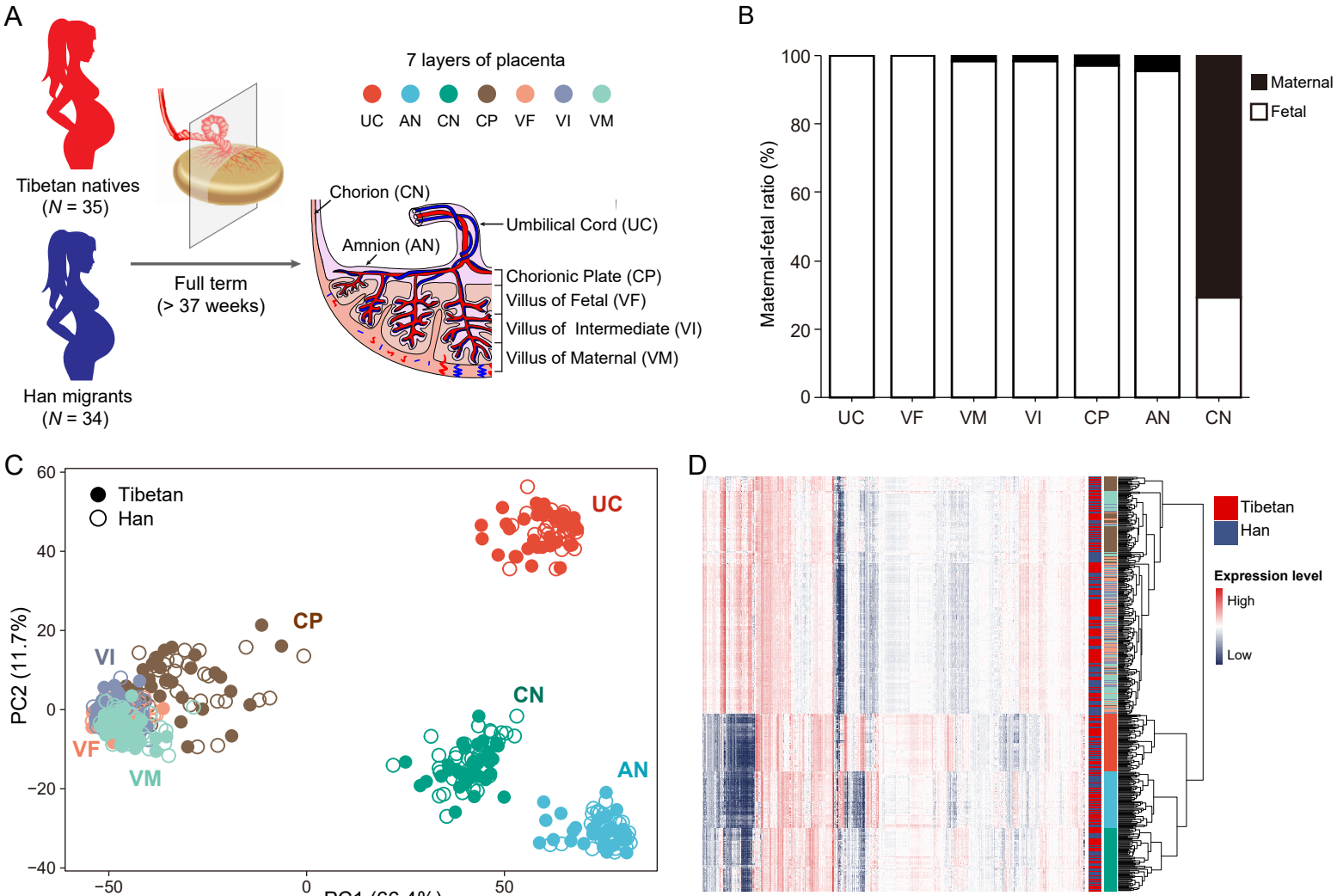
A
Tibetan natives
(N = 35)
Han migrants
(N = 34)
Full term
(> 37 weeks)
7 layers of placenta
UC AN CN CP VF VI VM
Chorion (CN)
Amnion (AN)
Umbilical Cord (UC)
Chorionic Plate (CP)
Villus of Fetal (VF)
Villus of Intermediate (VI)
Villus of Maternal (VM)
B
Maternal-fetal ratio (%)
Maternal
Fetal
UC VF VM VI CP AN CN
C
Tibetan
Han
PC2 (11.7%)
PC1 (66.4%)
UC
CP
VI
VF
VM
CN
AN
D
Tibetan
Han
Expression level
High
Low

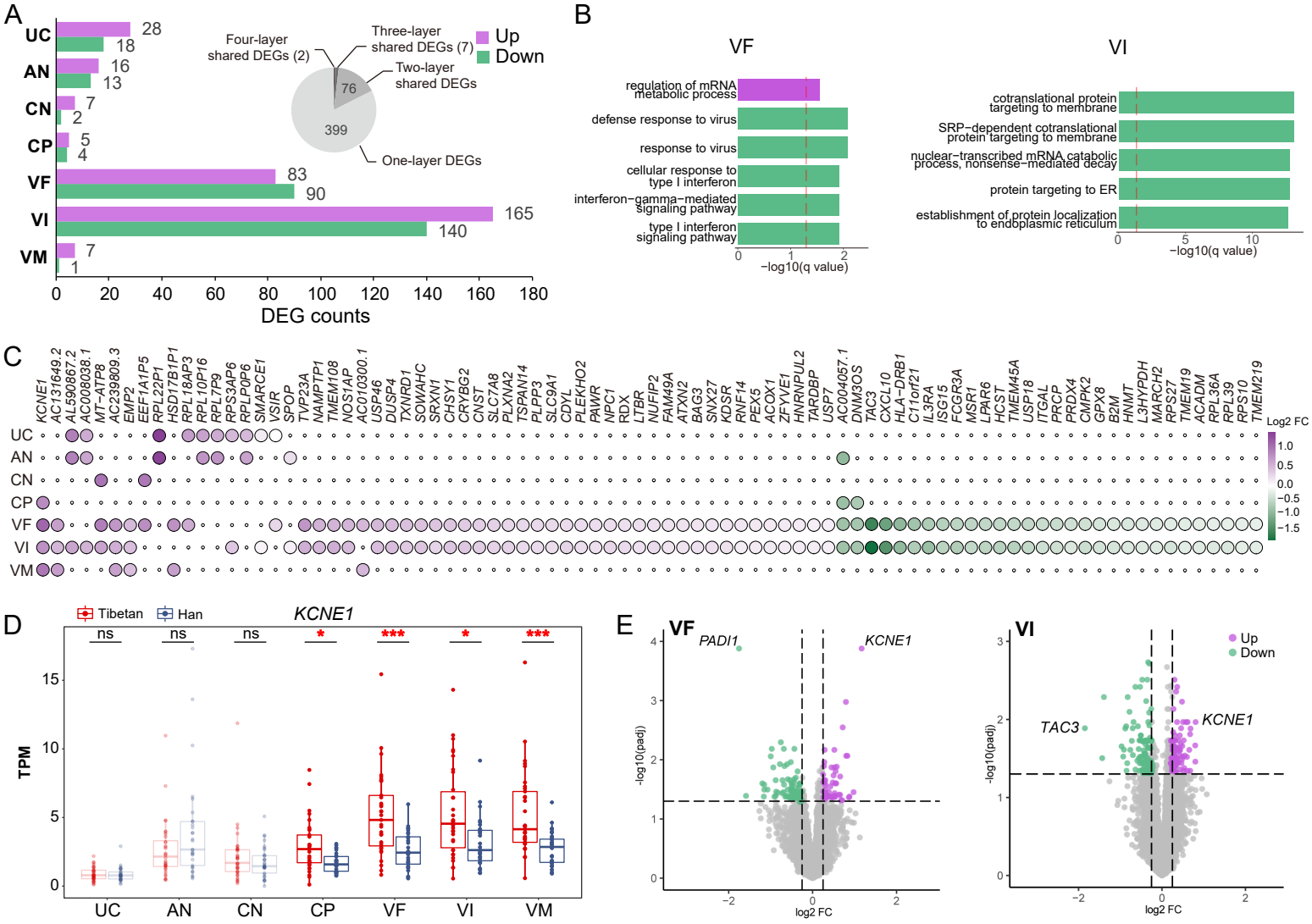
A
UC
AN
CN
CP
VF
VI
VM
28
18
16
13
7
2
5
4
83
90
165
140
7
1
0
20
40
60
80
100
120
140
160
180
DEG counts
Up
Down
Four-layer shared DEGs (2)
Three-layer shared DEGs (7)
Two-layer shared DEGs
One-layer DEGs
76
399
B
VF
regulation of mRNA metabolic process
defense response to virus
response to virus
cellular response to type I interferon
interferon−gamma−mediated signaling pathway
type I interferon signaling pathway
−log10(q value)
VI
cotranslational protein targeting to membrane
SRP−dependent cotranslational protein targeting to membrane
nuclear−transcribed mRNA catabolic process, nonsense−mediated decay
protein targeting to ER
establishment of protein localization to endoplasmic reticulum
−log10(q value)
C
KCNE1
AC131649.2
AL590867.2
AC008038.1
MT-ATP8
AC239809.3
EMP2
EEF1A1P5
RPL22P1
HSD17B1P1
RPL18AP3
RPL10P16
RPL7P9
RPS3AP6
RPLP0P6
SMARCE1
VSIR
SPOP
TVP23A
NAMPTP1
TMEM108
NOS1AP
AC010300.1
USP46
DUSP4
TXNRD1
SOWAHC
SRXN1
CHSY1
CRYBG2
CNST
SLC7A8
PLXNA2
TSPAN14
PLP3
SLC9A1
CDYL
PLEKHO2
PAWR
NPC1
RDX
LTBR
NUFIP2
FAM49A
ATXN2
BAG3
SNX27
KDSR
RNF14
PEX5
ACOX1
ZFYVE1
HNRNPUL2
TARDBP
USP7
AC004057.1
DNM3OS
TAC3
CXCL10
HLA-DRB1
C11orf21
IL3RA
ISG15
FCGR3A
MSR1
LPAR6
HCST
TMEM45A
USP18
ITGAL
PRCP
PRDX4
CMPK2
GPX8
B2M
HNMT
L3HYPDH
MARCH2
RPS27
TMEM19
ACADM
RPL36A
RPL39
RPS10
TMEM219
UC
AN
CN
CP
VF
VI
VM
Log2 FC
1.0
0.5
0.0
−0.5
−1.0
−1.5
D
Tibetan
Han
KCNE1
ns
ns
ns
*
***
*
***
TPM
15
10
5
0
UC
AN
CN
CP
VF
VI
VM
E
VF
PADI1
KCNE1
-log10(padj)
log2 FC
VI
Up
Down
TAC3
KCNE1
-log10(padj)
log2 FC

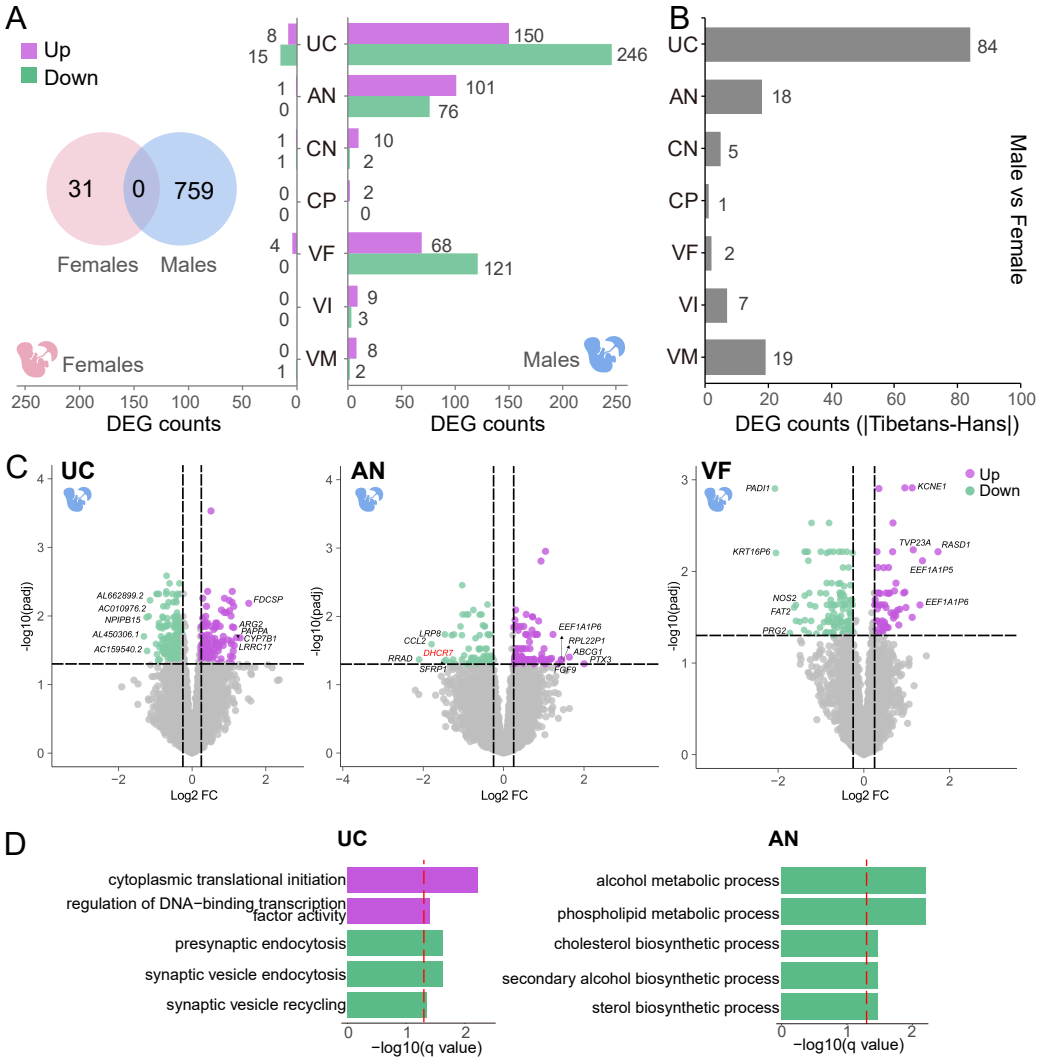
A
Up
Down
31
0
759
Females
Males
UC
AN
CN
CP
VF
VI
VM
8
15
150
246
1
0
101
76
1
1
10
2
0
0
2
0
4
0
68
121
0
0
9
3
0
1
8
2
Females
Males
250 200 150 100 50 0
0 50 100 150 200 250
DEG counts
DEG counts
B
UC 84
AN 18
CN 5
CP 1
VF 2
VI 7
VM 19
Male vs Female
0 20 40 60 80 100
DEG counts (|Tibetans-Hans|)
C
UC
AN
VF
Up
Down
-log10(padj)
Log2 FC
AL662899.2
AC010976.2
NPIPB15
AL450306.1
AC159540.2
FDCSP
ARG2
PAPPA
CYP7B1
LRRC17
LBP8
CCL2
DHCR7
RRAD
SFRP1
EEF1A1P6
RPL22P1
ABCG1
PTX3
FGF9
PADI1
KCNE1
KRT16P6
TVP23A
RASD1
EEF1A1P5
NOS2
FAT2
EEF1A1P6
PRG2
D
UC
cytoplasmic translational initiation
regulation of DNA−binding transcription factor activity
presynaptic endocytosis
synaptic vesicle endocytosis
synaptic vesicle recycling
−log10(q value)
AN
alcohol metabolic process
phospholipid metabolic process
cholesterol biosynthetic process
secondary alcohol biosynthetic process
sterol biosynthetic process
−log10(q value)

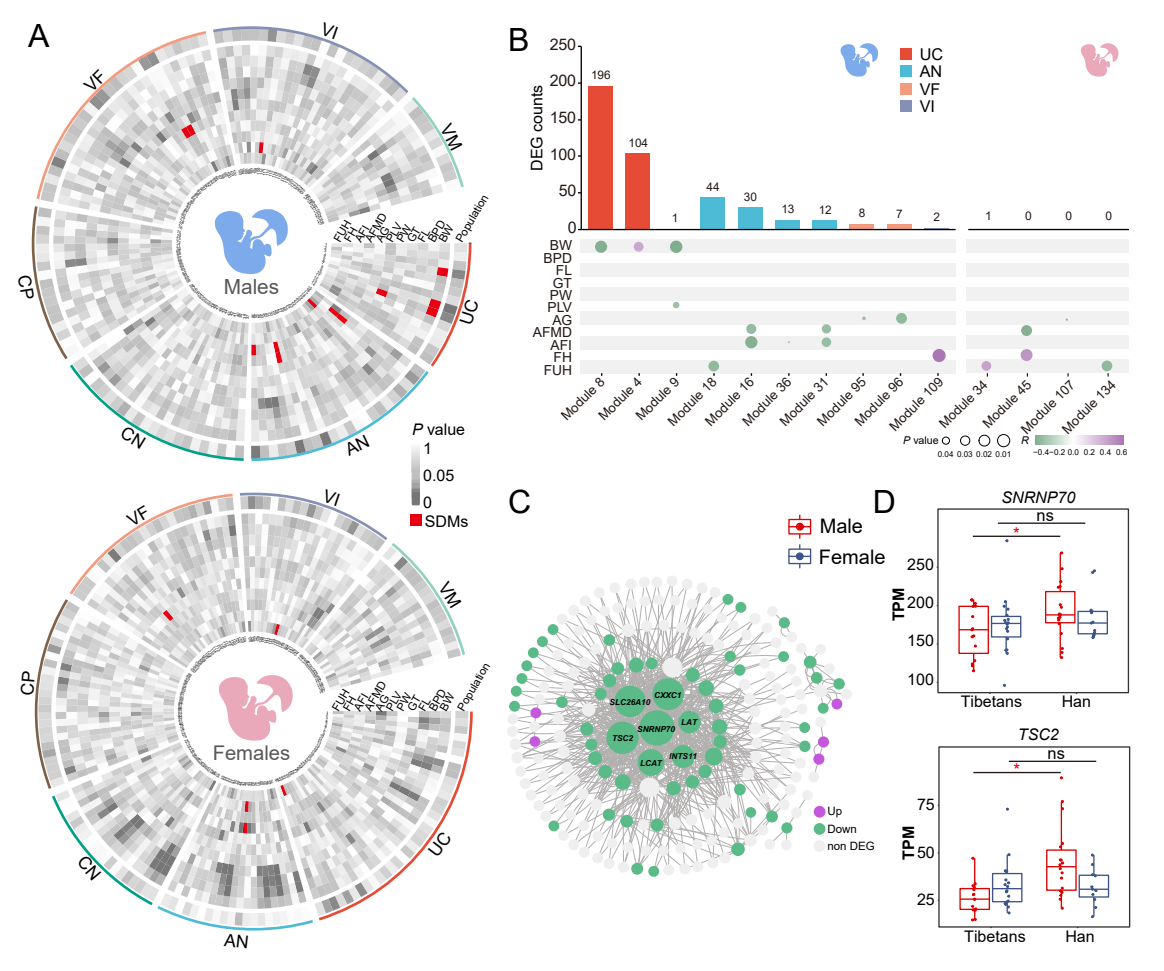
A
VI
VM
UC
AN
CN
CP
VF
Males
Females
FUH
FH
AFI
AFMD
AG
PLV
PW
GT
FL
BPD
BW
Population
P value
1
0.05
0
SDMs
B
DEG counts
UC
AN
VF
VI
196
104
1
44
30
13
12
8
7
2
1
0
0
0
Module 8
Module 4
Module 9
Module 18
Module 16
Module 36
Module 31
Module 95
Module 96
Module 109
Module 34
Module 45
Module 107
Module 134
P value
R
C
Male
Female
SLC26A10
CXXC1
LAT
SNRNP70
TSC2
INTS11
LCAT
Up
Down
non DEG
D
SNRNP70
ns
TPM
Tibetans
Han
TSC2
ns
TPM
Tibetans
Han

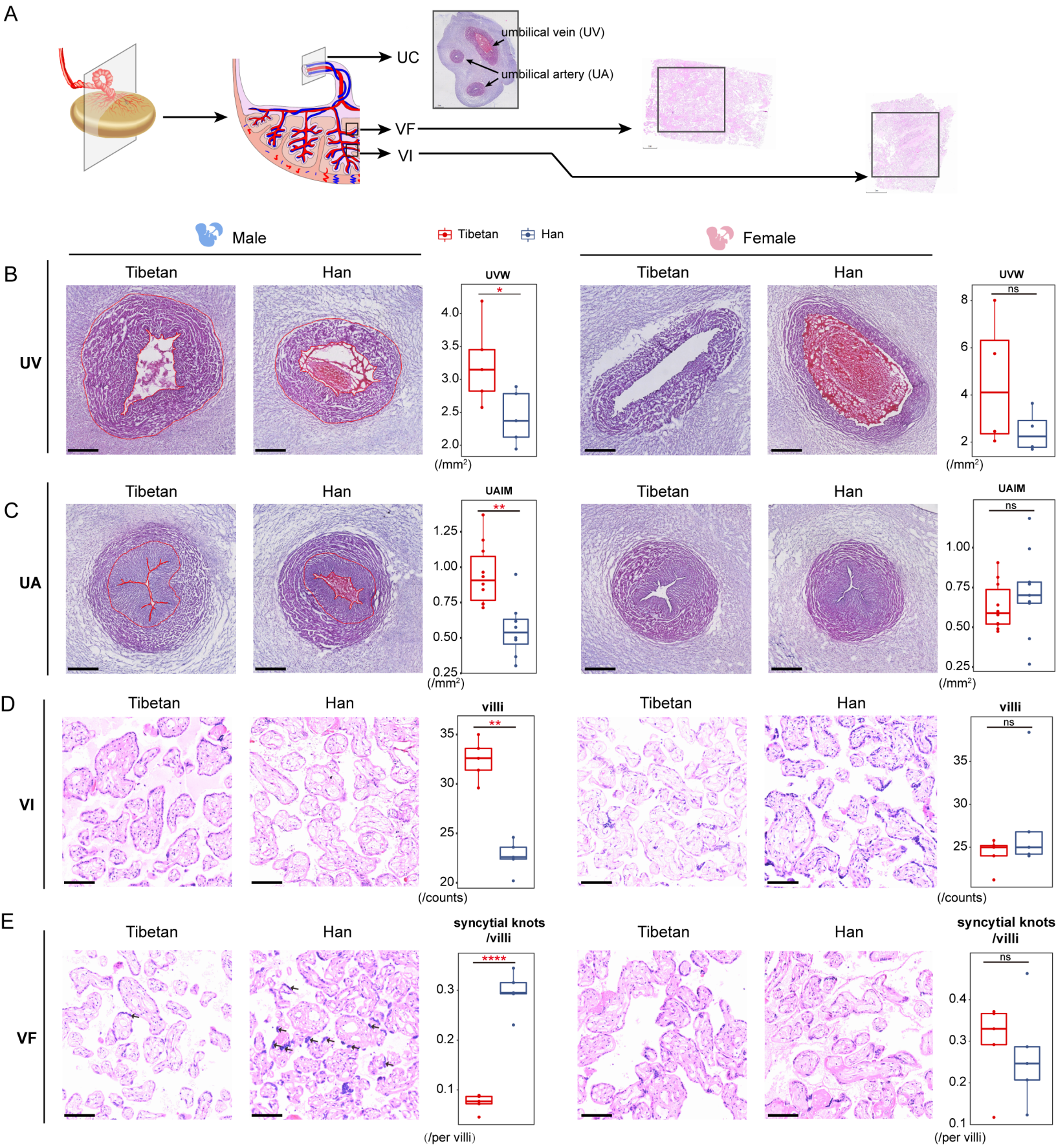
A
UC
umbilical vein (UV)
umbilical artery (UA)
VF
VI
Male
Tibetan
Han
Female
B
UV
Tibetan
Han
UVW
*
ns
(/mm²)
C
UA
UAIM
**
ns
D
VI
villi
**
ns
(/counts)
E
VF
syncytial knots /villi
****
ns
(/per villi)

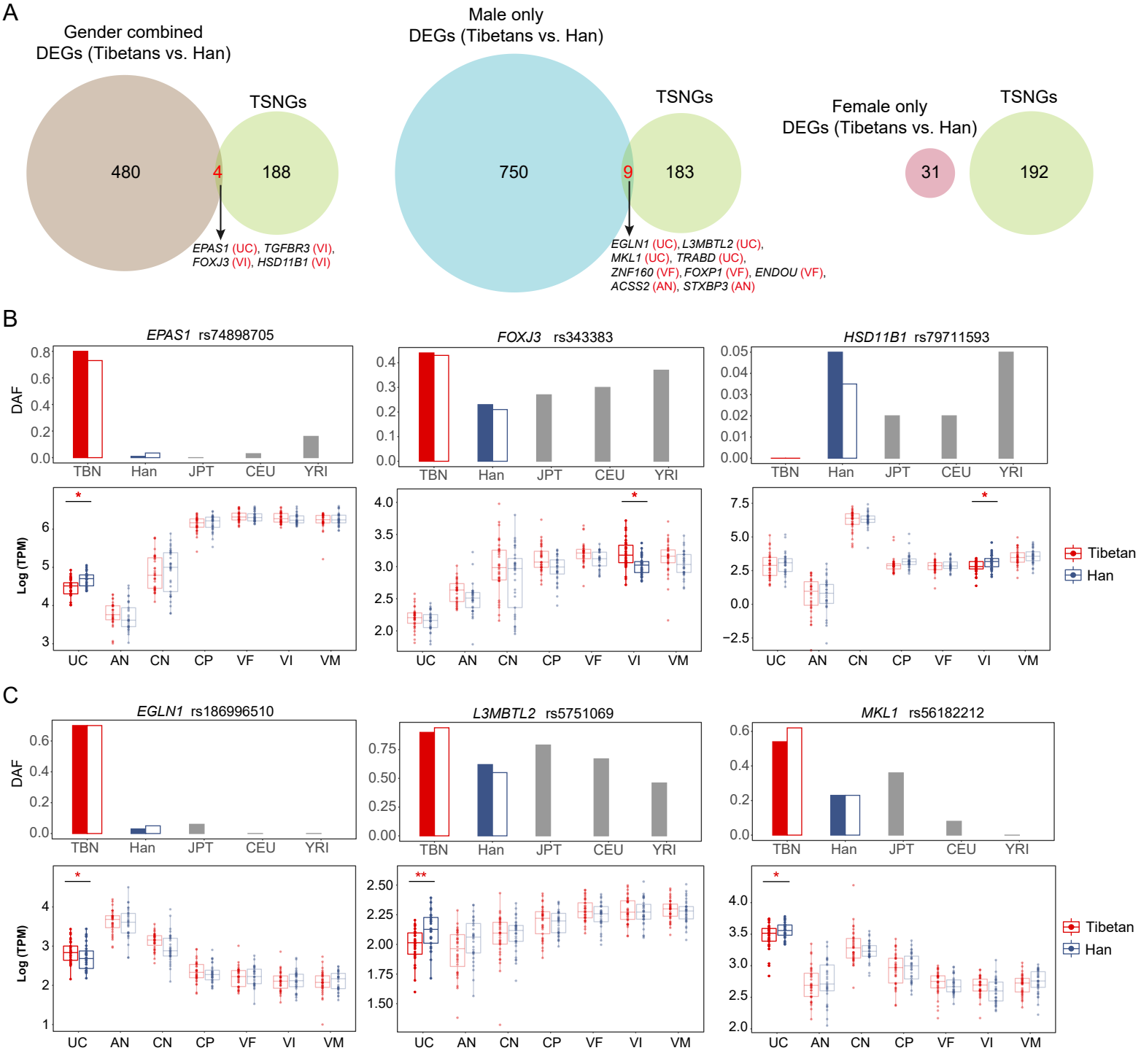
A
Gender combined
DEGs (Tibetans vs. Han)
TSNGs
480
4
188
EPAS1 (UC), TGFBR3 (VI),
FOXJ3 (VI), HSD11B1 (VI)
Male only
DEGs (Tibetans vs. Han)
TSNGs
750
9
183
EGLN1 (UC), L3MBTL2 (UC),
MKL1 (UC), TRABD (UC),
ZNF160 (VF), FOXP1 (VF), ENDOU (VF),
ACSS2 (AN), STXBP3 (AN)
Female only
DEGs (Tibetans vs. Han)
TSNGs
31
192
B
EPAS1 rs74898705
FOXJ3 rs343383
HSD11B1 rs79711593
DAF
TBN
Han
JPT
CEU
YRI
Log (TPM)
UC
AN
CN
CP
VF
VI
VM
Tibetan
Han
C
EGLN1 rs186996510
L3MBTL2 rs5751069
MKL1 rs56182212
DAF
Log (TPM)
Tibetan
Han